Universidad de Valladolid

UNIVERSIDAD DE VALLADOLID

ESCUELA DE INGENIERIAS INDUSTRIALES

Grado en Ingeniería Electrónica Industrial y Automática

A Comparative Study of Different Induction Motor Signals for Condition Monitoring Purposes

Autor:

Ferreras Blanco, Julia

Responsable de Intercambio en la Uva:

Moríñigo Sotelo, Daniel

Universidad de destino:

Università degli Studi di Pavia

Valladolid, Julio de 2022.

TFG REALIZADO EN PROGRAMA DE INTERCAMBIO

TÍTULO: A Comparative Study of Different Induction Motor Signals for Condition Monitoring Purposes

ALUMNO: Julia Ferreras Blanco

FECHA: 8 Julio 2022

CENTRO: Facolta' Di Ingegneria

UNIVERSIDAD: Università degli Studi di Pavia

TUTOR: Lucia Frosini

ACKNOWLEDGEMENTS

This final degree work puts an end to my stage as a grade university student. It has been five years of hard work, effort and dedication to this branch of engineering.

During this time, I have not only learned concepts about this science, but I have also been formed as an adult, dealing with heavy workloads and pressure, which thanks to the support and help of my family and friends, has been possible to confront easily these situations.

I will highlight here the people I cannot forget, since their support has been essential during my venture.

I would like to start with my mother and father, who had been always beside me, taking care, and supporting every of the decisions I have made, always believing in me.

My two lovely grandmothers (Julia y Carmelita), remembering me where I am, and what I'm worth.

My friends (Javier, Silvia, MJ, Olivia, Ana, Linda), who have helped me, and support me; remembering me that not always is going to be easy the path chosen to reach a goal.

To my project tutors (Daniel Moríñigo Sotelo and Lucia Frosini), and laboratory colleagues, without whom there would be no been possible to carry out the project, with which I have learned a lot.

At last but not least, my two brothers (Carlos and Javier), giving me lessons of kindness and happiness, even in worst times.

Just thank you all.

ABSTRACT

The main objective of this work is to identify and to understand the meaning of the different signals of an induction motor, being able to detect whether and where an abnormal behavior can exist, once the different faults have been studied.

Another objective is to study the different parts that compose a test bench, installed in the laboratory of the University of Pavia, in Italy. With the three-phase induction motor (model RAEL RL 90L 4), some tests have been carried to understand the different parts of an induction motor, and how it operates depending on the load applied to it.

KEYWORDS

- Induction motor
- Harmonic spectrum
- Slip
- Power
- Broken Rotor Bars

INDEX

FIGURE INDEX

TABLE INDEX

1. INTRODUCTION AND DESCRIPTION OF OBJECTIVES

1.1. Brief state of the art

Electrical motors are used in most of the machinery. Their low size allows to create high-power machines even in little volume, for example in household appliances such as a blender or a drill. Also, their high torque and high efficiency make them the ideal solution for the traction of heavy transports, such as trains, as well as the propulsion of ships, submarines and mining dumpers, through the diesel-electric system.

The squirrel cage motors are the most used, thanks to their low failure rate. These motors are sturdy and tough, requiring a low maintenance. Also, this maintenance has been improved through new techniques to evaluate early faults in these types of motors, to reduce the chances of creating damage into the motor. This type of maintenance is called predictive, performed by monitoring different physical variables of the motor, using different types of sensors. The most commonly used signals are stator current, vibration, and stray flux.

The objective of this project is to analyse the different signals obtained from the different graphs, from the test bench to evaluate and understand what different signals mean, and whether an abnormal condition could exist or succeed.

1.2. Description of the final degree project objectives

The objectives initially proposed for this project, are the following:

Learning objectives:

- Understand the different types of asynchronous motor and how they work
- Understand the spectral analysis
- Get different information of the various faults that can happen in the asynchronous motors
- Acquire knowledge of signal sampling

Specific objectives:

- Description of a new test bench assembled at the electrical machines laboratory of the University of Pavia.
- Performance of some lab trials with this test bench collecting some signals from a healthy induction motor.
- Understanding different signals obtained from the motor

- Learning and using spectral analysis to analyse and compare the spectra of these signals.

2. THEORICAL BACKGROUND

2.1.The Induction Motor

Electric motors are machines that transform electrical energy into mechanical energy. Within the different existing electrical machines, in this work the induction motors, also known as asynchronous motors will be explained in detail.

The induction motor is a type of electric motor, in which the alternating current in the rotor is generated by the magnetic field produced by the stator coils. (Fernández Villafañez, 2018)

Induction motors are made of two principal parts: the stator and the rotor. They are both placed in a form that the internal cavity of the stator pack and the external surface of the rotor, are reconditioned to correct any imperfections and to ensure a perfect centering of the rotor, forming the air gap, with an order of 0.3 to 3 mm approximately.

The rotor with the stator forms the electric circuit. The magnetic circuit is composed by the magnetic flux between the stator, the rotor, and the air gap. (Martín-Riva, 2014)

2.1.1. Stator

The stator is the stationary element that is fixed in the housing. It is formed by:

- Insulation materials: like resin, or polyamide.
- The stator winding: enameled copper wire coils, shifted by 120 degrees (three phase).
- Structural iron-silicon of the stator: packing iron-silicon sheets (usually non-grain oriented).

Figure 1: Stator windings (Frosini, 2022)

2.1.2. Rotor

The rotor is mounted on an axis and rotates.

- Structural iron-silicon, of the rotor: packing iron-silicon sheets (usually non-grain oriented).

The magnetic field will create an electromagnetic force in the rotor, which makes it rotate, at a speed (n).

In order to facilitate the dissipation of the heat produced by power losses, the housing is almost always finned and a fan is mounted on the shaft. *(Frosini, 2022)*

2.1.2.1. Rotor Types

Squirrel Cage Rotor

In this type of rotor, the three-phase winding is formed by aluminum or copper bars, enclosed at their ends to two rings, causing a short-circuit between them.

This type of motor is very common, thanks to the very low price, and its facility to use.

This rotor does not have a number of poles of its own, but the induced currents circulating in the bars, generate as many poles as there are in the rotating inductor field. (Fernández Villafañez, 2018)

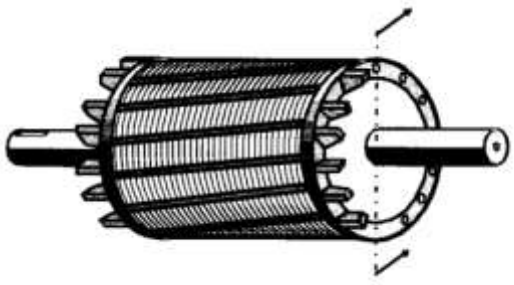

Figure 2: Squirrel cage rotor

This squirrel cage motor can be made in two ways according to the power generated.

For great power, a copper bar is inserted for each slot. Electrical and mechanical enclosure is achieved by two front rings into which all bars are connected with couplings and welds.

For lower or medium power, this rotor can be made by die casting; by filling the slots with pressure cast aluminum alloys or copper.

Figure 3: Squirrel Cage rotor (Frosini, 2022)

2.1.2.2. Double Squirrel Cage

A particular type of squirrel cage motor has a rotor with two concentric cages, called the outer and inner cage; made as a solution to improve the characteristics at the start-up of the motor.

The stator of this motors is a conventional three phase, but the difference stays in the rotor, that is made up by two cages with the same numbers of bars. (Frosini, 2022)

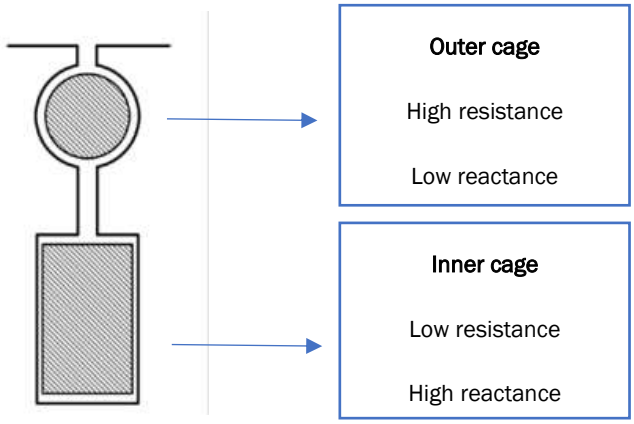

Figure 4: Double squirrel cage scheme

The outer cage (situated close to the airgap) has less section that the inner one, and can be made up by a material with a high resistivity like bronze. On the other hand, the inner cage is made up by a material with less resistivity, like copper, with the objective of making a higher resistance in the external cage. Nevertheless, often the material of the two cages is the same (generally aluminum).

Between both cages there is thin slit, made to increase the leakage flux of the inner cage, since the field lines of flux have a path with lower magnetic reluctance, Figure 5. The external cage has a lower leakage flux, direct consequence of being next to the

airgap, because the field lines have to include higher proportions of airgap, with a higher reluctance.

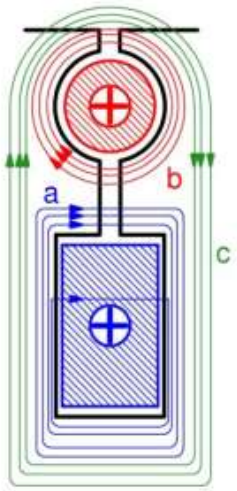

Figure 5: Leakage magnetic field lines through a double squirrel cage (Rodíguez Pozueta, 2018)

The principle of working of this double squirrel cage leads on the formula:

$$f_2 = sf_1 \tag{1}$$

Where f_2 is the frequency of the currents of rotor, and f_1 is the frequency of the currents of the stator. In the startup, the slip takes the value 1, making both frequencies at the same value, and the reactances reach their highest value. Therefore, in the startup the external cage, despite having greater resistance, has less impedance than the internal cage (of high reactance and, consequently, a greater impedance), and the rotor currents preferentially circulate through it. This achieves a high starting torque, since the rotor then presents a high resistance.

As the rotor speed increases, the frequency f_2 becomes lower and the currents go through both cages, increasing the current in the inner cage, which reactance decreases, and reducing the current in the external cage. During nominal operation, the reactances become close to zero, and all the current goes through the inner cage, because it has lower resistance.

In conclusion, when the slip takes lower values (nominal working), the value of the reactance is close to zero, and the values of the impedances are given by the

resistances. So, as the external cage has greater values of resistance, normally the current will flow through the inner cage. (Rodíguez Pozueta, 2018)

2.1.2.3. Wound Rotor Motor

In this rotor, the copper wire coils form the three-phase winding, with round or rectangular conductors. These conductors have to be insulated between them, and between the slots where they are packed.

This motor uses two types of slots: the open ones, with the characteristic that the conductors can be easily inserted, however it increases the magnetic reluctance. And the other type is the semi closed slots, that are more used because they do not increase the reluctance previously mentioned.

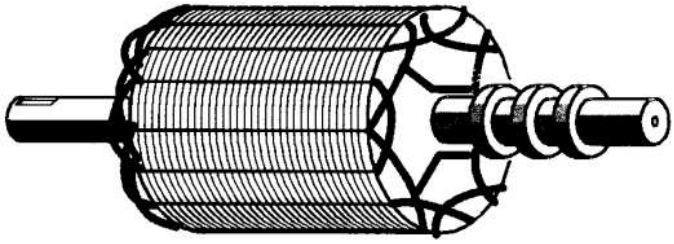

Figure 6: wound rotor (Fraile Mora, 2003)

This rotor needs to have the same polarity number as the stator.

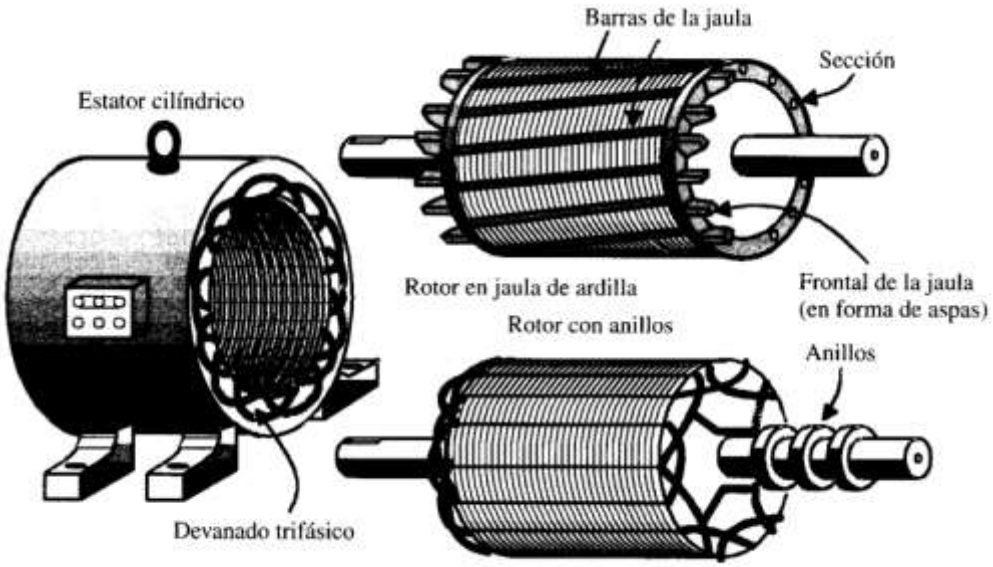

Figure 7: Types of rotors (Fraile Mora, 2003)

2.2.Torque-speed characteristics of the motor

To explain the values obtained from the realized test, with the objective to known the different parameters of the motor, and to examine the different characteristics of the motor, firstly, the torque-speed characteristics of the motor will be explained briefly. (García Santamaría, 2017)

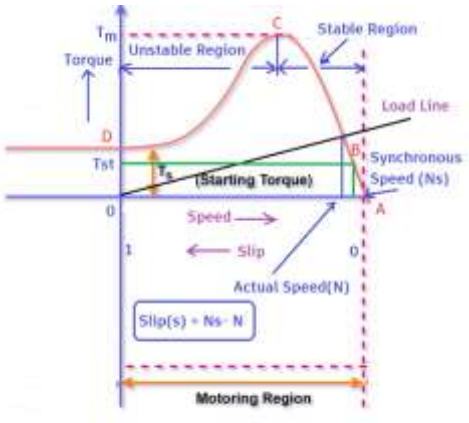

Figure 8: Torque-speed curve

There are three different working zones of the machine, according to the slip parameter. When the slip takes a value higher than one, the machine will be working as a brake. When the value of the slip is in the range between zero and one, it will be working as a

motor; and finally, the region where the slip takes values smaller than zero, the machine will be working as a generator.

In the case of study, it will be studied the asynchronous machine working in the motoring region, (presented in Figure 8). This region represents the most characteristic working mode, with slip range values between 0 and 1.

The most characteristic points, presented in the Figure 8 in red color, of this motoring region, are:

- Point A: Synchronous operation: $s \approx 0$, $T \approx 0$: In this case the rotational speed of the motor would be close to the synchronous speed. The torque is also close to zero.
- Point B. Nominal regime: $s=s_n$, $T=T_n$: This torque value is fixed by the manufacturer as ideal work value. The speed that the motor develops at this point is known as nominal speed.
- Point C. Maximum Torque operation: $s=s_m$, $T=T_m$: It is the maximum torque that the machine can develop, and is given at the critical speed ($n_{critical}$).
- Point D. Start-up, $s = 1$: The speed is zero and corresponds to the starting torque.

An interesting point of this curve is that the maximum torque (point C) divides the curve into stable and unstable region. All tests in the laboratory, have been carried out in the stable region of the machine. (de la Torre)

2.3. Different classes of Asynchronous motors

The American Association law called NEMA (National Electrical Manufacturers Association) has created an identification with letters, for every squirrel cage induction motor, according to determinate electric and mechanical construction design. (The engineer toolbox, 2022)

The classification created from NEMA, according to the design of the squirrel cage rotor, is:

Design	Starting torque (% Full Load Toque)	Maximum Torque (% Full Load Toque)	Starting Current (% Full Load Current)	Slip (% synchronous speed)
A	160 (normal)	230	500-800 (normal)	<2 (low)

B	140 (normal)	200	500-600 (normal)	<4 (low)
C	225 (high)	180	(low)	<5 (low)
D	275 (high)	-	(low)	5-8, 8-13% (high)

Table 1:classification according to NEMA of squirrel cage motors

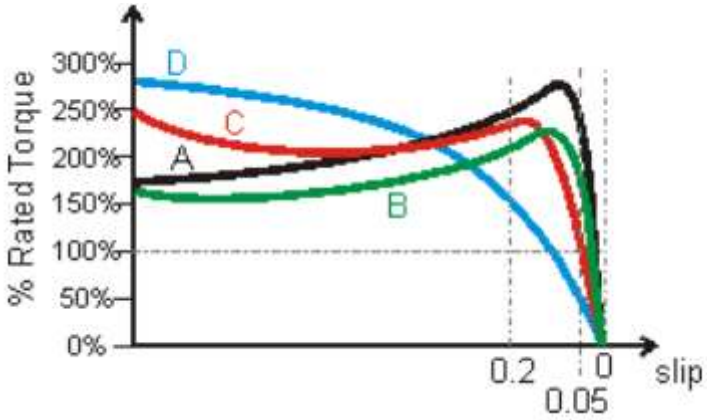

Figure 9: sketches of NEMA-class a-d torque speed curves (SCHULICH SCHOOL OF ENGINEERING, 2022)

NEMA Class A- normal starting torque, Normal starting current, Low slip. The shape of the squirrel cage rotors leads to a normal, close to the nominal, starting torque. Working in normal conditions the resistance is low, and the current can flow equally. Also, the low slip, makes better working conditions to reach a high efficiency, being an indicate motor for general purpose. (Alvizu, 2022)

NEMA Class B-Normal starting torque, Low starting current. The starting torque is close to the nominal one. In working conditions, the slip is low, making a good efficiency. The application of this motor is similar to the class A, general purpose. It is mainly used for constant-speed drives where the starting torque is not severe such as pump, blowers and machine tools.

NEMA Class C-High starting torque, low starting current. Normally these rotors have a double squirrel cage, developing a high starting torque, and a low starting current. Because of the high starting torque, the value of the acceleration is elevated, resulting adequate motor for heavy startup loads, like piston pumps or compressors.

Under heavy loads, the time working is limited by the thermal dissipation, which makes this rotor the most suitable for large sudden loads with low inertia.

NEMA Class D-High starting torque, high slip, low startup current. This type of motor combines a high torque, meaning a higher resistance, with a high nominal slip. Normally two types of design are presented according to the slip (5-8% and 5-13%); when the slip is higher than 13%, they are called ultra-high slip.

This motor is developed to work under intermittent loads involving high acceleration duty and for driving high-impact loads such as presses and shears. In some cases, the motor is supported into a flywheel which helps supply the impact and reduces the pulsations in power drawn from the supply system.

In essence, according to NEMA, class A and B squirrel cage motors have a low resistance, and are adequate to prioritize the nominal work. The bars of these rotors have a huge section, but the ones for class B are the largest ones, making these motors the more used. The classes C and D rotors are more suitable for starts-ups, rather than nominal work. Class C, allows a very high start-up thanks to the double squirrel cage, and class D also allows a very high torque for the start-up, but with the inconvenient of a higher resistance. Also, D class is the less accurate for nominal working conditions, cause takes a higher slip, and the resistance becomes higher to work; also, the efficiency will decrease substantially. (SCHULICH SCHOOL OF ENGINEERING, 2022)

Determination of the class of the motor according to NEMA

In the Figure 10 the different values of the motor from the laboratory are represented, only taken below the maximum torque, in the stable region. Comparing this graph to the ones from NEMA, the characteristics of the motor are close to the class A or B. The slip is here represented in percentage.

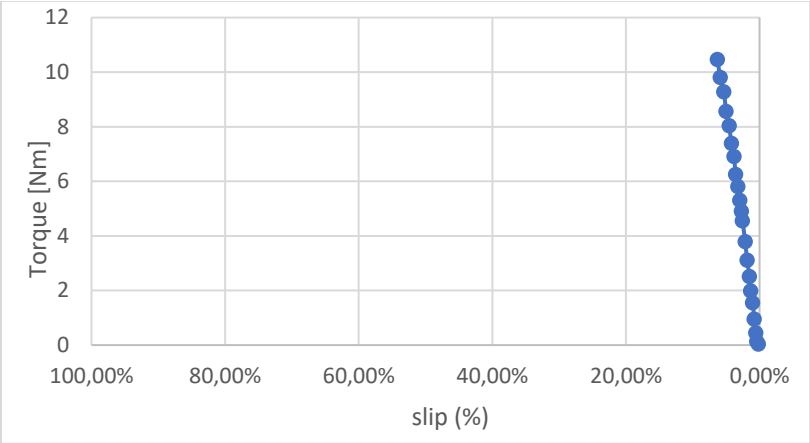

Figure 10: graph Torque-slip

To make concrete the class of the motor, an illustration of the different rotor bar shapes is presented:

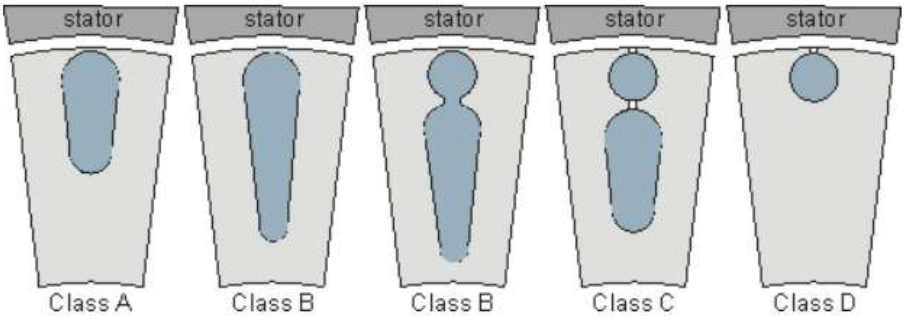

Figure 11: illustration of rotor bar shapes for different motor classes

Finally, an illustration on the stator and the rotor shapes of the RAEL motor is shown (Figure 12); taking a look to the bars of the rotor, the shape is more similar to class B.

Figure 12:Image of the rotor given by RAEL

2.4.Faults of an Induction Motor

2.4.1. Introduction

An induction motor presents some characteristics like being a simple, hard and cheap.

Nevertheless, it should not be said that this motor does not suffer from its operation. Working in the range zones settled by the manufacturer should not cause any damage to the motor; but if one of the stresses on the motor exceeds the nominal range, it will make the life of the motor briefer, sometimes inducing a catastrophic damage. This is the main reason why it is important to evaluate the preventive diagnostics of an induction motor. (Lee, 2021)

Reliability of machine and components depends on machine structure, rating applications, and operating environment. For smaller machines, the fault percentages are:

- Bearing related (41%): rolling element, raceway, lubrication system…
- Stator related (36.5%): ground insulation, wedges, core, frame…
- Rotor related (9.5%): core, cage, shaft…
- Others (13%)

In this chapter the main faults related to rotor, stator and the bearings of an induction motor are shown. Also, some common failures that affect all the machine are presented.

2.4.2. Rotor Faults

Thermal Stresses

Thermal stresses develop from high anomalous temperatures in the rotor. Between them, there are:

Thermal overload

It can cause damage during the shutdown, start-up, and during normal operation.

This type of fault can be detected visually in the rings and the bars of the rotor.

This thermal stress is caused for example, by:

- High number of start-ups consecutively
- Shutdown of the rotor with high load.
- Insufficient ventilation
- Broken bars

Thermal unbalance

It is the increase of uncommon temperature, caused by operating out of the work ranges. It can be caused in both; shutdown, and start-up.

The common causes are:

- Hot points in the surface of the rotor.
- Temperature gradients caused by a bad ventilation
- High number of start-ups consecutively
- Different heating between the bars and the core of the rotor.

The consequences of this high temperature can be the break of the bars, and the rings, and the separation of the bars attached to this ring. (López Tello & Bedoya Arango, 1997)

Heat points and excessive loss

During the fabrication there are some variables that can lead on losses, and hot points.

- Wrong connections from the bars to the ring
- Inappropriate design
- Non-uniformity in the distribution of the lamination
- Misalignment between the bars of the rotor and the lamination

There are some probes with the aim of detect the majority of this problems, like ultrasonic testing, commissioning for open or broken bars. Also measuring noise, vibration, temperature, current can help to check the health of the rotor.

Sparks on the rotor

There are two types of sparks in the rotor, can be destructive or non-destructive.

The non-destructive can appear in the normal operation mode of the rotor, although they are not normally seen, because of the low intensity.

The destructive one, occurs mainly in the starts-up, direct consequence of the high current.

Another type of sparks, are the ones allocated in the air gap, that are in fact, tiny particles produced in the core. If these particles have been produced during the assembly, will disappear in time. On the other hand, if the particles have been produced by the sparks, these will last the whole live of the motor.

Electromagnetic Stresses

These stresses are due to magnetic causes, and the effects caused by the noise and the vibration due to electromagnetic forces.

Electromagnetic effect

The magnetic flux which interacts with the current, produces electromagnetic forces capables of performing vibrations in the bars This vibration can lead to fatigue, fracture

of the bars. If the vibration is excessive the sparks appear making erosion. These vibrations are higher in the start-up.

Unbalanced Magnetic fields

Normally the rotor of an induction motor is not precisely located in the centre because it may have some misalignment. This leads to two different parts, differentiated by the distance between the rotor and the stator. In the zone where the distance between these two parts is smaller, a smaller reluctance will exist, making a higher magnetic field. In the zone with more distance the magnetic field will be smaller. This creates a misalignment of forces, and can even cause the bending of the axis, and as a result, the stator and the rotor will be in contact.

Noise and electromagnetic vibration

Some elements with the function to create a magnetic field do not contribute in the same way, generating some vibration and noise; for example, if the rotor and the stator are not on the same axis.

Mechanical Stresses

Airgap Eccentricity

It is the uneven distribution of radial airgap. There are two types of eccentricity: the static and the dynamic. The static eccentricity is the result of core ovality, manufacturing tolerances, and incorrect installation, for example. On the other hand, the dynamic eccentricity is the result of bent shaft, and asymmetric thermal expansion between others. Also, mixed eccentricity can happen, as the result of both issues together.

Rotor cage failure

Generally, it occurs in motors with frequent starts or large load variations attributable to large thermo-mechanical stress; for example, radial thermal expansion of end rings, or axial thermal expansion of rotor bars. The results are cracks or detachment in bars, additional vibration, loose bar, intermittent arcing between rotor core and loose bar and a protrusion of rotor bar. (García Santamaría, 2017)

2.4.3. Breakage of Bars of the Rotor

As previously explained, the rotor is made up by some bars joined in their extremes by rings, called short-circuit rings. All together is called cage. The magnetic core of the rotor is made up of a series of insulated and stacked magnetic sheets, which occupy the space between the bars. The cage of the rotor is built with aluminum or copper, in such a way that both bars and rings are cast inside the rotating magnetic package.

In the bars of the rotor, one of the most common failures in the induction motors is breakage and cracking, especially in the motors that start-up under load.

In the start-ups the current that flows through the bars is greater, because the speed of the rotor is much slower than the speed of the stator. These currents induce an increase of the temperature and an expansion of the bars, since the difference between the electric resistance is in the individual bars. This warm-up together with the expansion will not be qual for every bar, producing cracking in the bars. When a crack appears, the resistance of the bar increases, which further increases the heating, worsening the crack condition.

Once the crack has appeared the process degenerates, the faulty bar heats up around the crack to the point of breaking, the breakage causes the appearance of electric arcs between the two separated parts, which usually damage the magnetic circuit.

Meantime the close bars will receive higher currents and higher mechanical and thermal efforts, because of the low current in the cracked bars.

These cracks normally start in points where the bar is not hold by the rotor, that is in the proximities of the joints with the short-circuit ring or in the short-circuit ring itself, and parts that suffer from higher mechanical stresses of the structure.

In the process of the malfunction development, it must be considered that the rotor bars support the braking and acceleration forces of the motor; therefore, if the machine undergoes abrupt variations in its speed, originated during its during its working cycle, the failure can develop quickly as a result of material fatigue.

2.4.4. Stator Faults

Thermal Stresses

Thermal overload

It emerges when there is a temperature extremely high, due to a deficient ventilation system, frequent start-ups, variation of the supply voltage.

Thermal expansion

Following the Montsinger Law, with an increment of 10ºC of the working temperature, the life of the machine can be reduced to almost a half. The duration of the insulation can be calculated with the Arrhenius law:

$$L = Ae^{-bT} \quad (2)$$

Where: L is the calculated life in hours; A and b are constants depending of the thermal class, and T is the temperature.

Inter-laminar insulation failure

It is the gradual weakening of the mechanical and dielectric strength of interlaminar insulation due to motor operating stresses, like thermal overloading. The consequences are melting or burning of laminations, propagation of the fault, and motor failure between others.

Figure 13: interlaminar insulation failure (Lee, 2021)

Mechanical Stresses

Movement of the coils

In machines working with low or high voltage, during start-up, high currents are developed and electromagnetic forces are originated in the coils. These forces produce damage in the insulation, from little fragments, to important dismemberments.

Fatigue produced by vibrations

The vibrations that are present in this type of machines, makes in time a reduction in life. In case of bad fastening, the coils can be affected also by the vibrations, and produce frictions with other parts.

Introduction of external objects

It can happen that an external object intrudes in the air gap, affecting the correct operation of the stator and the rotor. Also, the insulation can be damaged, producing damage in the coils, bars and rings.

Magnetic Wedge Failure

In case of magnetic wedges, due to the iron content, the mechanical strength is feeble. It causes mechanical stresses, like stator winding and wedge vibration, thermal stresses, wedge thermal expansion and contraction; and other like loosening, breakage and disintegration of magnetic wedges.

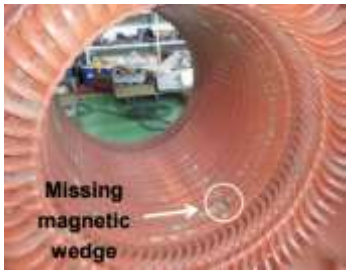

Figure 14 (Lee, 2021)

Partial discharges

In the manufacturing process some voids can appear in the airgap. As a consequence, the evaporation of the volatile components from the insulation, takes part in process like defective impregnation, loss of insulation capacity or delamination. When these voids, with the action of the electric circuit, exceed the dielectric constant of the air, they can produce little discharges, producing a degradation of the airgap, even puncturing it.

Tracking effect

It is known as the creation of superficial roads, or alternative paths, that drive the current to the ground. This current circulation degrades the airgap continuously. It is aggravated by dust, dirty and humidity.

Electric transient

There are over voltages produced in a very short time, that can damage seriously the insulation. They are consequence of a voltage difference between phases, continuous starts-ups and commutation periods.

Dielectric hysteresis

It contributes to losses in the air gap in form of heat. When the produced heat is higher than the dissipated, leads to a localized increase in temperature, that can perforate the insulation.

Corona effect

It is an electrical discharge promoted by the ionization of a fluid surrounding a conductor carrying a high voltage, and it is manifested in a form of luminous halo. Because the conductor normally has a cylindrical shape, this halo is manifested with the shape as a crown, and that is why the name of the phenomenon. This effect is caused because the molecules composed by air get ionized, and are capable to drive electric current. This leads to an increment of the temperature, and the color of the halo will change, so the color can indicate the temperature experimented. (Wikipedia, 2022)

Environmental Issues

Contamination and Condensation

The dust particles, the water, the oil can enter through the ventilation, making in time a layer of dust, leading in a worse dissipation of the heat from the motor, decreasing the life of it, even reaching the breakdown.

Extreme Environmental Temperature

In both cases, when the temperature can be extraordinarily high or low, the machine can result damaged. In the first case, if the temperature is extremely high and the machine is working in normal conditions, there is an increase in the temperature of the windings, leading into a deterioration in the insulation of the stator. On the other hand, when the temperature is very low, it can create problems of condensation, making necessary a system to eliminate the condensate water.

2.4.5. Bearing Faults

A bearing is a machinery component that plays an important role, since it dominates the machine performance. If one of the bearing fails, the machine and the test bench (in this thesis), can be damaged. This requires the most careful use and maintenance of these parts.

The problems of the bearing normally are in the outer or inner race, in the balls, or in the cage.

Lubricants are used between contact surfaces to keep the parts in continuous motion, with the aim to reduce the friction among rolling and sliding surfaces. There are also other aims like heat dissipation, removal of particles and contaminants, corrosion protection among others. (RKB, 2010)

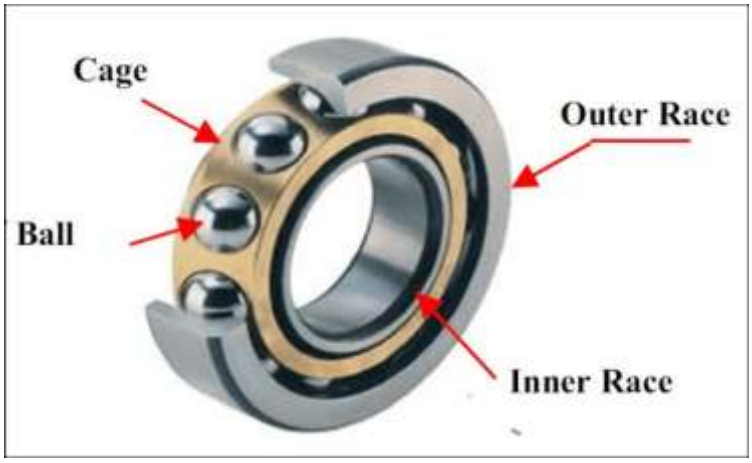

Figure 15: rolling element bearing: simple structure, ease of replacement, low friction, low reliability (Research Gate, 2022)

The failure process is indicated normally by an increase in noise, vibration, or heat; producing accelerated mechanical wear. Also, microscopic surface fractures are produced, due to cylindric loading stresses. (MRO Machinery and equipment , 2022)

Lubrication

The most common failure in bearings is the improper lubrication. Some factors such as operation load, speed and temperature, determinate what kind of oil or grease is needed.

It is important to know when it is time for renewing lubrication, and how much lubricant is necessary, in order not to damage the elements. This cause can produce premature bearing failures, and most of them can be avoided.

In the image showed below, it can be seen that almost the 80% of the damages are result of the improper lubrication.

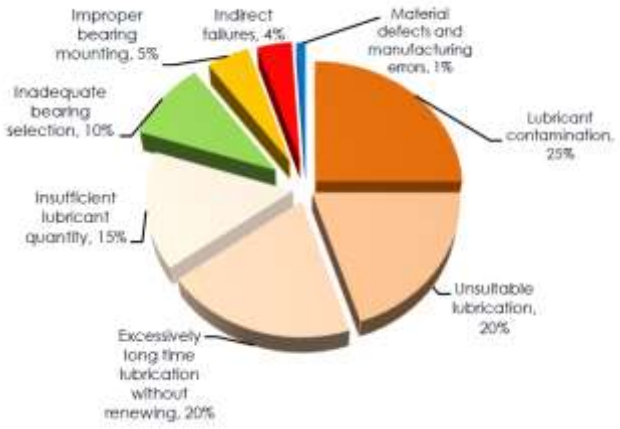

Figure 16: - Common bearing failure causes in % (RKB, 2010)

Inadequate bearing selection

Normally, the selection of the bearing is imposed by the manufacturer, which is the most adequate; but it can be changed, once all the possibilities are studied. Nevertheless, it is not always a good solution.

Another mistake is choosing a larger bearing, with the chance of increasing the radial load capacity. But this creates additional problems, like for example a lower speed than the nominal, and the motor cannot not work properly.

Normally, the changes of the bearing require the same exact model, to get a good efficiency.

Improper mounting

Although the percentage produced by improper mounting is low, with a total of 5%; certainly, it is always a cause of damage, leading to a bearing failure in misalignment, or improper load distribution.

A tiny misalignment in the mounting of the bearing is enough to arise obstacles in vibration and temperature, causing non-parallel running problems. These problems produce heavy wear in the ball or roller pockets where they run, between others.

These non-parallel running problems can be seen into the mark of the ball on the outer raceway.

Figure 17: Bearing failure due to improper mounting (RKB, 2010)

Another problem is the excessive or uneven heating of the bearing, when it is mounted on shaft of the housing; the heat moved to the inner ring must be less than 125°C, in most cases; and it is important to demagnetize the bearing before the installation, just to avoid the attraction to various ferrous metal particles.

Indirect failures

These failures represent approximately 4% of the total of premature bearing failures. Together with other cases, the worst operating conditions are overloading, excessive vibrations, and high temperature.

Overloading introduces plastic deformation at the rolling elements and raceway contacts, forming shallow depressions or flutes in the raceways, in the pitch of the rolling elements.

Figure 18: Plastic deformation on an inner ring raceway produced by overloading (RKB, 2010)

During equipment operations, electrical discharge may produce a high level of static electricity, dissipated by the bearing to the ground, resulting in pits or fluting. Initially the issues will take the form of craters, and then flutes will develop from these craters in time.

Figure 19: Craters formed by current leakage resulting in fluting (RKB, 2010)

Stray magnetic fields generate high electrical currents, that passing through bearing, also produce some injury.

While in the stationary, vibration introduces what is called false brinelling. This damage can produce either brightly polished depressions or reddish stains. These marks are equal to the distance between the rolling elements.

Ineffective sealing

The use of incorrect seal material leads to a contamination from different external agents, that can cause serious damage in the bearing; for example, failure due to water contamination.

In steel, due to the water, oxidation takes place in the surface, and the formation of corrosion pits occurs, followed by a flaking in surface.

Figure 20: Bearing failure due to water contamination (RKB, 2010)

2.5.Maintenance Procedures

Maintenance consists in the actions carried out with the objective of checking the correct conditions, in which the object can operates normally.

2.5.1. Preventive Maintenance

The preventive maintenance is the one that requires frequent revisions, time-based maintenance, according to the expectancy life of the component, trying to avoid malfunctions. This is the most effective maintenance, reducing or avoiding collapses.

The main tasks are for example: change different components, cleaning, inspection…

This maintenance not only reduces damages, it also reduces costs by about 60%, and the time outs; and improves the efficiency of the installations, extending the useful life of the installation, and improving the quality of the production.

However, the main problem is the fact of replacing the different elements before the end of their useful life. (DATADEC, 2022)

2.5.2. Corrective Maintenance

This type of maintenance consists in repairing or replacing the fault, once it has occurred in the installation. It does not require previous analysis, only when the fault appears it is repaired, with qualified personnel.

The corrective maintenance requires more expensive reparations, due to the fact that the cause normally induces collateral damage, that would not happen with the preventive maintenance.

Also, it creates an unwanted sub-activity in the enterprise, as a result of the unprepared shutdown of the failed machine and the machines related to it. (DATADEC, 2022)

2.5.3. Predictive Maintenance

This maintenance makes use of different techniques to detect working anomalies and potential defects,

in the different components of a machine, to solve the problem before it occurs.

It is based on tracking the status of the equipment, and through periodic test results, obtains the condition of the machine and, if necessary, notifies about the anomaly.

Some of the advantages related to this type of maintenance are, for example, the unnecessary disassembly, a worth use of the useful life of the components, finer planning, between others.

The disadvantages are a major cost in qualified personnel, and techniques to detect the failures. Also, some of the indications given can be false, a false alarm or a missed fault. The false alarm causes unnecessary inspection; and on the other hand, the missed

faults cause failures without any prior indication, and a potential forced outage. Both false alarms rely into high cost and loss of production. (IBERDROLA, 2022)

2.6.Analysis of the power

In electrical machines, there is a transformation from electric energy into mechanical energy, transferred from the stator to the rotor through the airgap, with some unavoidable losses.

First the power absorbed by the induction motor from the grid is the result of:

$$P_1 = m_1 V_1 I_1 \cos\varphi \tag{3}$$

Where V_1 is the voltage of each phase, I_1 the current of each phase and φ the offset between them.

This power arrives to the stator, but in there some power losses occur, caused by the Joule effect or the effect of the iron (later explained in detail).

Hereafter, the power that arrives into the rotor through the airgap called Pa, is:

$$P_a = P_1 - P_{cu1} - P_{fe} \tag{4}$$

Also, in the rotor the losses by the Joule effect are notable, so the power transmitted into the axis, called mechanical power, is:

$$P_{mi} = P_a - P_{cu2} \tag{5}$$

Definitely, the useful power is:

$$P_u = P_{mi} - P_m \tag{6}$$

Where P_u is the useful final power, and P_m is the loosed power related to friction and windage. (Figure 21)

The diagram below represents a scheme of the powers:

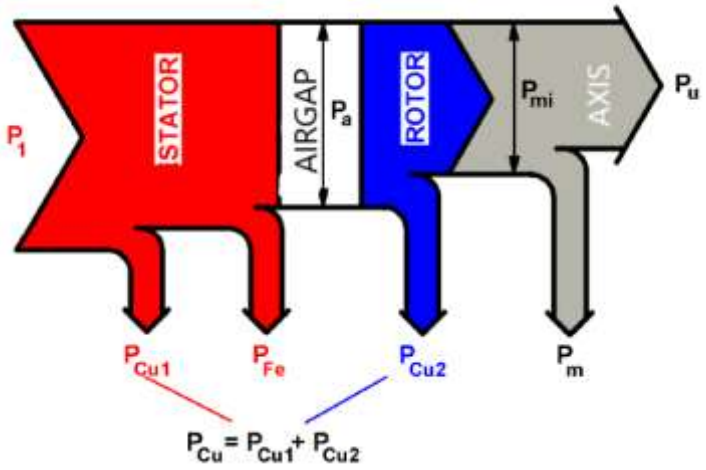

Figure 21: energy dissipation flowchart

The effects of the losses in the power

To evaluate the power and the losses of the motor, it is necessary to calculate the power transmitted from the stator to the rotor, and the losses occurred in the process. (Fraile Mora, 2003)

The principal losses are for example the **Joule effect losses**, that occurs in the stator and the rotor, depending on the resistance and the current. These losses can be dependent or independent of frequency. The independent ones are related with the diameter and the characteristics of the material used, and other factors like the temperature or the place of the work. The dependent losses are due to skin effect. The skin effect refers to alternating electric current in a conductor, affecting the distribution of the density in the conductor. The current density decreases exponentially from the surface towards the inside This reduces the effective cross-section of the conductor and increases its effective resistance.

The following equations can be used to define the Joule losses:

- Stator:

$$P_{cu1} = m_1 R_1 I_1^2 \tag{7}$$

- Rotor:

$$P_{cu2} = m_2 R_2 I_2^2 \tag{8}$$

Where m_1 and m_2 are the number of phases.

Another important loss is **caused by the iron.** These losses are caused by the hysteresis effect, by parasitic currents and additional losses. These losses are directly affected by the weight and the frequency, this means that these losses increase with the dimensions of the motor. This type of losses is only counted in the stator, because it depends on the frequency. The frequency of the rotor is the result from the frequency of the stator multiplied by the slip. Normally the slip, takes very low values, making these losses are negligible compared to the stator values.

$$P_{Fe} = m_1 E_1 I_{Fe} \tag{9}$$

Where I_{fe} refers to the current flowing thought the iron.

The last are the **mehanical losses**, related with friction and windage. They depend directly on the speed. The friction losses depend specially on the bearings, that must be perfectly lubricated. The windage losses increase when the dissipation of the heat is not enough.

Measurement of the power in the laboratory

To obtain this power and efficiency measurement in the laboratory, an experimental test has been carried out.

The efficiency of the motor is defined as:

$$\eta = \frac{Pout}{Pin} \times 100 \tag{10}$$

Where P_{out} refers to the power produced by the motor, and P_{in} refers to electric power, given from the grid to the test bench. These powers are calculated as:

$$P_{out} = speed\ (rad/s) \times torque\ (Nm) \tag{11}$$

$$P_{in} = P_1 + P_2 + P_3 \tag{12}$$

P_{in} is the sum of the power of the three different phases of the motor.

With the results taken from the experiment, the electric power is calculated by each of the three phases given by the wattmeter; and the output power can be obtained through

LabVIEW, from the parameters of the motor. It is simple to obtain the percentage of the efficiency of the motor.

The graph below relates the efficiency to the speed. As the speed of the rotor decreases, the efficiency of the motor increases. This is due to the fact that, as the input voltage increases (making a higher load) the power given from the grid to the motor increases, and the difference between the input and the output power experiments a growth, because there is more load and the losses increment. But this difference is lower in percentage, and the efficiency increases.

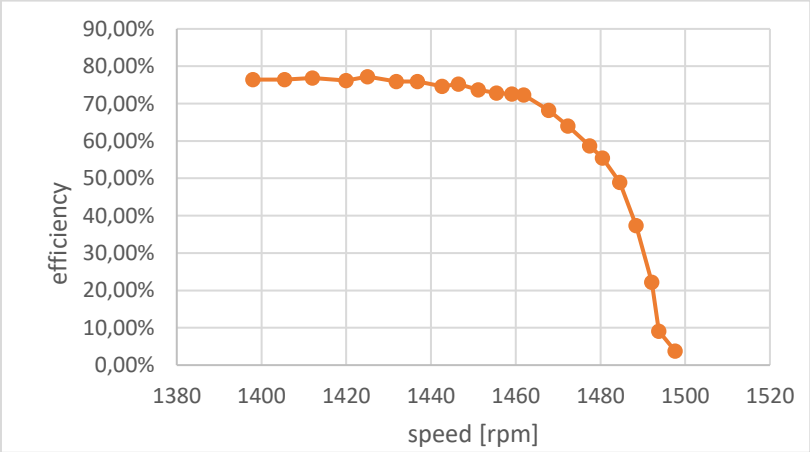

Figure 22: graph efficiency-speed

The value of the mechanical power given by the induction motor is the result of the product of speed and torque. In the graph below, the power decreases if the rotor speed increases. When the speed is near the synchronous one, the power is close to zero, because the torque has a very low value of 0.029 Nm.

$$P_{out} = speed\ (rad/s) \times torque\ (Nm) \tag{13}$$

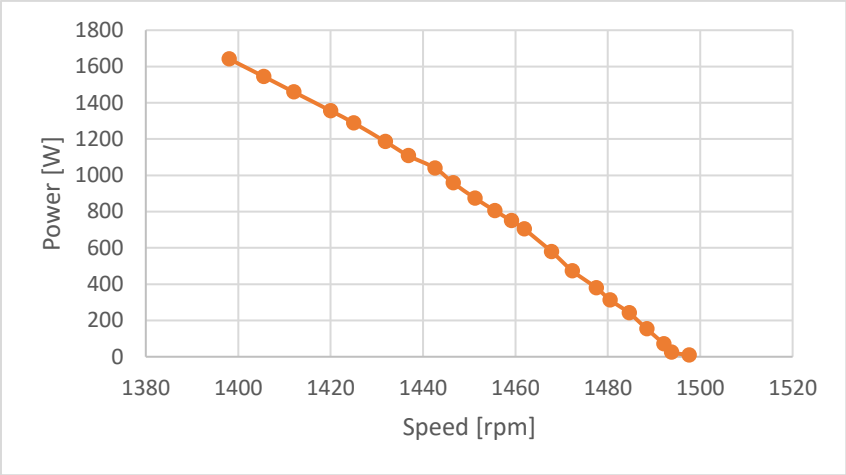

Figure 23: graph Power-Speed

2.7.The Measure of the Power

Electric power is the amount of electric energy delivered or absorbed by an element at a given time. The power can be divided in three types: active, reactive, and apparent power.

The Active power, also known as Real power (P) is consumed by resistive loads, and can be converted into another type of power (i.e. mechanical power in an electric motor). Reactive power (Q) is consumed by inductive loads or generated by capacitive loads, and cannot be converted into another kind of power. Lastly, Apparent power (S) is the power system´s ability to provide active and reactive power.

The units of power of real power are watts (W), for reactive power are vars (VAR), and for apparent power are volt-amperes (VA). (Aexander & Sadiku)

Active power is measured with a wattmeter. It gives an average power, in watts, of the instantaneous power over a period of time. Therefore, the formula to measure this input active power is:

$$P = V1I1\cos(\varphi 1) + V2I2\cos(\varphi 2) + V3I3\cos(\varphi 3) \quad (14)$$

This formula expresses the input power taken from the grid, to the stator. In it the power factor is shown, which expresses the ratio between the active power used in a circuit and apparent power delivered to the circuit

The second power is the **reactive power**. It represents the required power to create magnetic fields of the inductive elements, or electrostatic fields of the capacitive

elements. To calculate this power, an amperemeter (or ammeter), a voltmeter and a wattmeter, are necessary to measure the difference.

$$Q = V1I1\,\mathrm{sen}(\varphi 1) + V2I2\,\mathrm{sen}(\varphi 2) + V3I3\,\mathrm{sen}(\varphi 3) \quad (15)$$

At last, the **apparent power** is the result of the combination of active and reactive power. To calculate it, the Pythagorean theorem is applied, used in the power triangle, which states that the apparent power (S) is equal to the square root of the sum of the active (P), and reactive (Q) powers. (Tecnológico de Monterrey)

$$S = \sqrt{P^2 + Q^2} \quad (16)$$

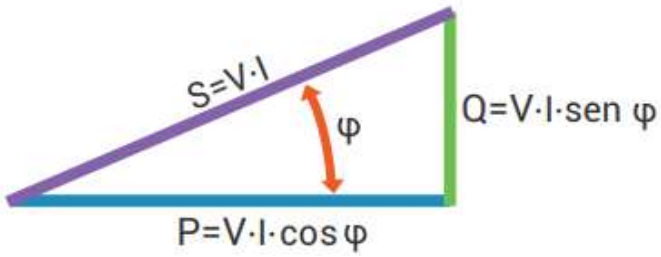

Figure 24: power triangle (Tecnológico de Monterrey)

Once the theory is explained, these concepts will be used in the laboratory.

To measure the active power in the laboratory, the wattmeter 304B from the brand Infratek, explained in detail in 3.2.10, is used. The scheme of the wattmeter is represented in the Figure 25.

It is represented by a three-phase system, without the presence of the neutral. The three phases are star connected.

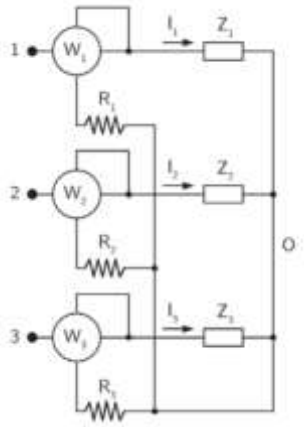

Figure 25: Scheme of the wattmeter (Magnaghi, 2015)

From the Wattmeter, the information given is the active power from every of the three channels (represented in the figure with W), and it represents the input power given from the grid to the motor. The sum of the three powers is realized to calculate the total active input power value. It also gives the power factor. (Malcovati)

In the values from the wattmeter, the uncertainty due to measurement errors, should be always taken on account, like wattmeter precision among others. This generates uncertainty in the measurement, the actual value should be between a range characterized by the uncertainty. In fact, it represents a range of values in which the actual value of the measure, is found.

To analyze the power factor, although, it has been previously mentioned that there is a power factor for each phase, the laboratory wattmeter only gives one power factor value, which is the mean of the three phases. When this parameter indicates 1, it means that the efficiency is the highest, on the contrary, values next to zero are ineffective.

The formula used to calculate the Power factor, is:

$$PF = \frac{True\ (active) Power\ (W)}{Apparent\ Power (\mathrm{VA})} \tag{17}$$

From this formula, the offset angle can be obtained as:

$$\varphi = \cos^{-1}(PF) \tag{18}$$

This angle gives the relation between the three different powers explained. This angle is represented in the Figure 24.

The results of the carried-out tests show that the values of the power factor, working always under the motoring region, decrease as the values of the speed are closer to the synchronous speed.

Also, the value is higher when the motor is working close to the nominal conditions, where the power gets its maximum value.

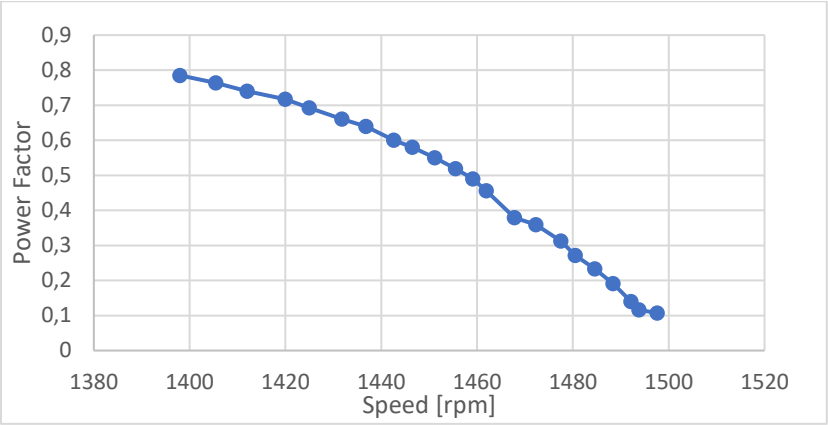

Figure 26: graph power factor-speed

In Figure 27, the relationship between the input and the output power given by the test bench is represented. As explained the input power is that given from the grid to the stator, and the output power is the power given by the motor (obtained by multiplying the speed of the rotor [rad/s] by the torque [Nm]).

The next graph shows the balances of the power, in the studied induction motor. When a load is applied to the motor, the input power required by the motor increases, generating more output power, and also increasing the power losses.

The greater demanded torque, the bigger is the power consumed by the motor and the power losses.

$$P_{in} = P_{out} + P_{losses} \tag{19}$$

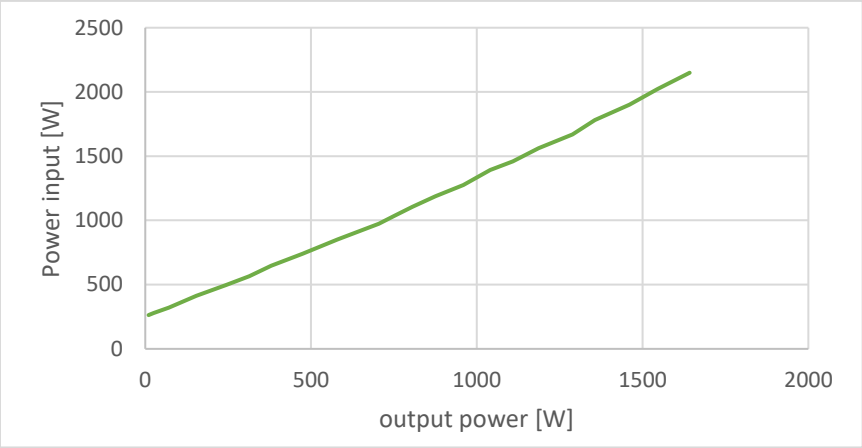

Figure 27: graph power input-output power

2.8.Fundaments of Spectral Analysis of Stationary Signals

2.8.1. Aliasing

Aliasing is an effect that makes the signals to come indistinguishable when are sampled, it is known as a frequency overlap.

2.8.2. Nyquist frequency

To avoid the effect of the aliasing, the frequency taken to recompose the signal from a sampled into a continuous one should be a least the Nyquist frequency (w_N). This frequency is calculated by dividing the sample frequency by two. (González Sánchez, 2022)

Frequencies above the Nyquist one appears as signals with low frequency.

To avoid the aliasing, it is necessary to eliminate all the signals with a frequency higher than the Nyquist one, before sampling it; for example, with a low-pass filter.

2.8.3. Quantization of Analogue Signals

The quantization takes place after sampling, used for taking amplitude values from an analogic signal, resulting a succession of discrete values.

During sampling, the amplitude is measured, and for each sample, a finite value is chosen, between a range of values previously selected.

This range of values depends on the resolution, and the numbers of bits used for the codification (n). As the number of quantization levels increase the quantization error decreases.

The number of quantization levels is 2^n (Moríñigo Sotelo, Pons Llinares, & Fernandez Cavero, 2021)

2.8.4. Harmonic Spectrum

From the Data Acquisition Board (3.2.9), the signals obtained like the current, voltage, flux, torque, are in the time domain. To obtain information from them, a conversion into the frequency domain is necessary. It can be done by many algorithms, but the most used is the Fourier Transform. (Moríñigo Sotelo, Pons Llinares, & Fernandez Cavero, 2021)

2.8.5. Fourier Transform (FT)

A common use to analyze the harmonic spectrum is the Fourier Transform.

This is a mathematical transform that allows to transform a function in time domain x(t), in a new function in the frequency domain x(ω)= x(2πf). This is a complex function made up of sinusoids that constitute the original function, and can be called frequency spectrum of the function x(t), or more commonly harmonic spectrum. (WIKIPEDIA, 2022)

This Fourier transformation is able to take the fundamental (the greatest weight in the configuration of the original signal) and the harmonics (multiples of the fundamental) from a time domain, converted into a frequency one.

Without going into too much analytical detail, it can be said that if the signal g(t) is a nonperiodic function in the time domain, then the corresponding transform is:

$$\hat{g}(f) = \int_{-\infty}^{\infty} g(t) e^{-2\pi i f t}\, dt \tag{20}$$

Where f denotates the frequency, and t denotates the time.

It is also possible, to trace the signal in the time domain from its Fourier transform in the frequency domain, with the formula:

$$g(t) = \int_{-\infty}^{\infty} \hat{g}(\omega) e^{-2\pi i f t}\, dt \tag{21}$$

The Fourier coefficients represent the amplitude of each harmonic-related sinusoid present in the Fourier series of a periodic function. (Magnaghi, 2015)

2.8.6. Discrete Fourier Transform (DFT)

This Fourier transformation is a type of discrete transformation, from the time domain into a frequency domain. It converts a fine sequence of samples, with a finite duration, into a sequence that is generated by sampling a continuous function.

From a series of N complex numbers x_0, ...x_{N-1} in the time domain, to a frequency domain, the DFT takes the form:

$$X_K = \sum_{n=0}^{N-1} x_n e^{-ik\frac{2\pi i}{N}kn} \quad (22)$$

Being K=0..., N-1.

Two main considerations give rise to spectral leakage:

- The signal has to be periodic T=N/fs (fs= sampling frequency)
- The frequency of the spectrum resolution is fs/N=1/T

Because the DFT is a sequence of number, it is ideal to process and use in digital applications.

2.8.7. Fast Fourier Transformation (FFT)

FFT is an algorithm to calculate the Discrete Fourier Transform, and its inverse. This algorithm has a lot of applications, for example the digital treatment of signals, and the filtration of some digital signals.

This algorithm reduces the complicacy of calculating, from the DFT that works with $O(N^2)$, to an easier way to calculate O(N log N), being N the total number of examples taken, to make the transformation. The main difference is the computational speed experimented, with a huge quantity of samples. (Magnaghi, 2015)

3. TEST BENCH DESCRIPTION

3.1.Introduction

In this chapter, the elements that compose the test bench used for carrying out the tests realized, will be presented and explained in detail, to understand and examine the different signals obtained from it.

This test bench can be found in the laboratory of the University of Pavia, in the department of Electric, Computer and Biomedical Engineering. Roughly, it is composed of three main parts, an induction motor, a brake and a torque sensor.

Firstly, to elaborate these different tests, there are two types of installations possible for the test bench: the supported and the suspended installation. The difference between them is the speed they can hold.

For low speed applications only, the suspended installation is adequate, where a single element coupling can be used. On the other hand, the supported installation is mandatory when a high speed is required.

In this case of study, the test bench has a supported installation.

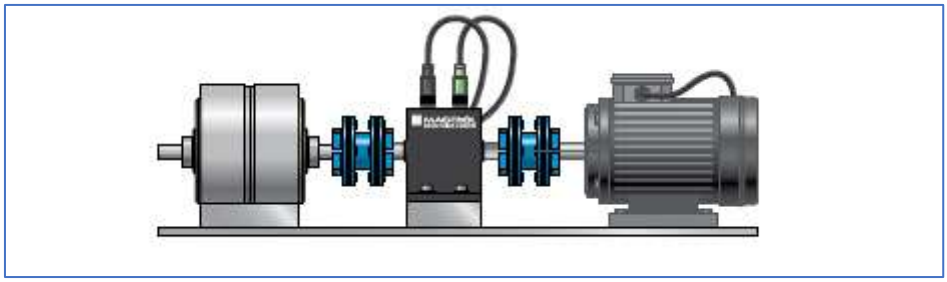

Figure 28: Supported installation scheme (MAGTROL)

One of the main objectives of the study is the signal of the torque. To acquire this information, a torque sensor will be used, from the MAGTROL company. This sensor is fixed to the motor and the brake, through couplings with two degrees of freedom.

An advantage of this type of installation is the possibility to increase the critical speed.

By contrast, some of the disadvantages, are a mayor length because of the use of the couplings, and an increased price.

Figure 29: Supported installation (laboratory photo)

There should be some precautions, like for example the alignment between parts conforming to the installation.

3.2.Parts of The Test Bench

3.2.1. Asynchronous Motor

The selected **asynchronous motor** to carry out the analysis is a three-phase induction motor, manufactured by RAEL (an Italian company), model RL 90L 4, with a certificate INERIS 05 AT EX 0025X.

As previously explicated, this type of motor consists mainly on a rotor, and a stator. In this case, the rotor of this machine is a type of squirrel cage, a set of bars parallel to the axial direction and arranged in cylindrical shape around the axis.

The motor RL 90L 4 has a total of 4 poles, i.e. 2 pairs of poles. In that case, the formula to calculate the synchronous speed is:

$$N_s(rpm) = \frac{60\left(\frac{s}{min}\right) * f\left(\frac{revolutions}{s}\right)}{Pp} = \frac{60\left(\frac{s}{min}\right) * 50\left(\frac{revolutions}{s}\right)}{2} = 1500\frac{revolutions}{min} = 1500rpm \quad (23)$$

However, synchronous speed cannot be reached at any condition, because there is a difference called slip, which marks the difference between the rotational and the synchronous speeds.

In the case the slip takes a null value, this implies that the variation of the magnetic field in the rotor is zero, and there is no induced electromotive force and no torque.

In the Figure 30 the speed indicated is 1400 rpm, which represents the speed at rated load. The speed will be always below 1500rpm.

The nominal characteristics at the working conditions of 400V/50Hz (with direct start) are:

Rated Power	1.5	[kW]
Nominal Speed	1400	[rpm]
Rated Voltage	230/400	[V]
Rated Amperage	6.6/3.3	[A]
Power Factor	0.8	-
Starting/nominal Current Ratio	5	-
Nominal Torque	10.4	[Nm]

Table 2: Characteristics of the motor RL 90L 4 RAEL. (Own elaboration, data obtained from RAEL)

Another information given by the manufacturer explains that this machine is able to operate at ambient temperatures between -20°C and +50°C. Also, to maintain good temperature conditions, it is air-cooled by an axial fan mounted on the shaft, to remove the heat produced during operation. The machine is of type Totally Enclosed Fan Cooled (TEFC). (RAEL)

At last, important details can be read directly from the nameplate of the motor, shown in the next figure:

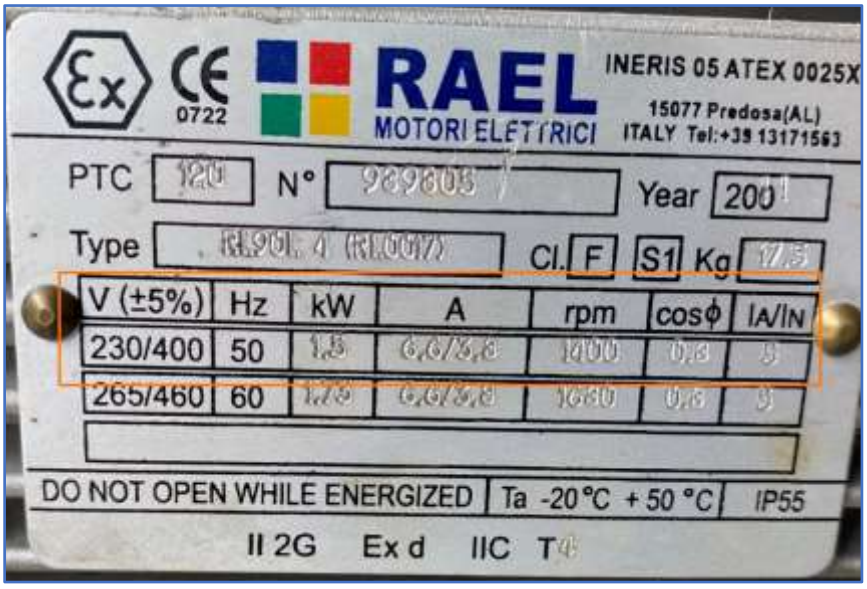

Figure 30: Nameplate of the motor (laboratory photo)

In the nameplate of the motor, two types of working conditions are presented. Each one corresponds to the conditions that are given from the grid. The American values use the 60 Hz, and European values work with 50 Hz. Knowing this, the selected row is the first one.

An important point that can be read in the nameplate of the motor is the duty cycle, known as the run and rest periods to which a machine is subjected (considering their duration and time sequence). The IEC 60034-1 explains ten types of duty cycle: indicated by a code with a letter “S”, followed by a number.

In the image above, the motor is a S1 type, this means a continuous duty, operation with constant load, during enough time to produce a thermal equilibrium. (Fraile Mora, 2003)

3.2.2. Motor Terminal Board

Another important characteristic in the asynchronous motor is how the terminals of the stator are connected. This is called the motor terminal box.

In this box the primary and the secondary terminals are shown, and they can be connected in two different ways, the star and the delta connection.

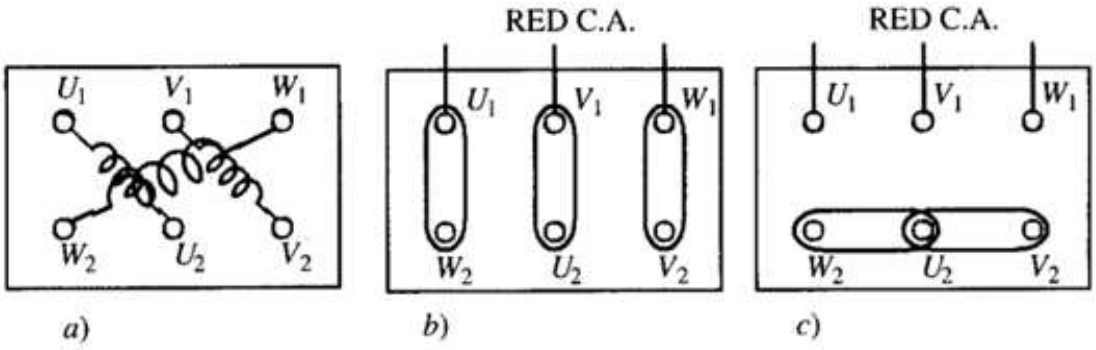

Figure 31: Motor terminal board, where b) is delta connection; and c) is star connection (Fraile Mora, 2003)

Figure 32: Motor terminal Board (Laboratory photo)

The photo taken at the laboratory shows the connection in a star type. This connection allows the machine to connect the highest voltage indicated in the nameplate of the motor, and the delta to connect the lowest voltage.

Particularly, taking a look to the image of the characteristics, it means that the power at 1.5 kW, with full load, and a speed of 1400rpm, can be reached by two ways. By a delta connection that needs a voltage of 230V, and 6.6; or, through the star connection, with a voltage needed of 400V, and a total of 3.3.

To invert the direction of rotation of the motor, it is only needed to change two wires, which are connected to the power supply.

3.2.3. Torque Transducer

Another element used in the test bench is the **torque transducer (TS 109/011),** giving an accurate torque and speed measurement.

This torque needs a power supply to give the corresponding measurement values. It is going to be supplied from a laboratory DC power supply, thanks to the analog connection. The values of the voltage should be between 12-32VDC, usually 24 VDC.

This transducer gives two outputs, which are an analog and USB. The USB is used to give digital information to the computer, and see information about the speed (rpm), and the Torque (Nm). This will therefore give the output power, by a simple multiplication between the speed and the torque (kW).

The refresh time of the continuous analog signals is 100 µs (10kHz). The USB interface will provide the data through the selected program called LABVIEW. (MAGTROL)

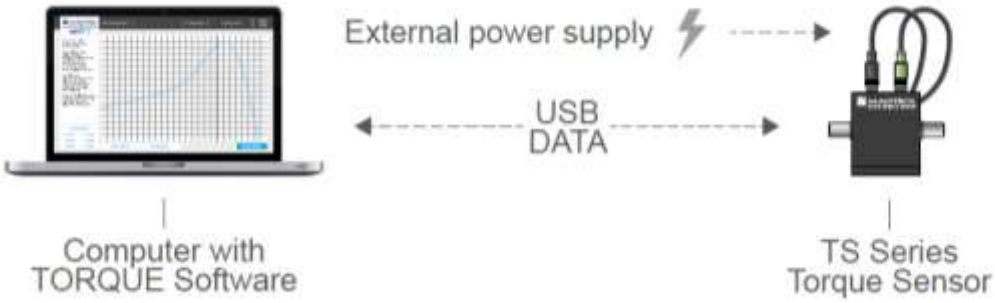

Figure 33: TS Torque Sensor USB only configuration (MAGTROL)

Figure 34: Torque transducer allocated in the laboratory (Laboratory photo)

The mechanical characteristics for the torque are:

(radial forces) F_r max	100	N
(axial forces) F_s max	300	N
Measuring range	20	Nm
Torsional stiffness	3600	Nm/rad
Inertia encoder side	9.100×10^{-6}	kgm^2
Inertia opposite side	2.23×10^{-6}	kgm^2
Inertia total	3.14×10^{-6}	kgm^2

Table 3: Characteristics of the torque (Own elaboration, data obtained from RAEL)

3.2.4. Couplings

When a torque transducer sensor is mounted, the type of lamellar joint is an excellent solution to the correction of the misalignment.

Two different couplings are used. One is stuck between the brake and the torque transducer. The other one is allocated between the torque transducer and the motor.

The first one (between the brake and the torque sensor) should hold high torsional stiffness, and high rotational speed, to improve the results from the test, and not damage the test bench.

This coupling consists of two dick packs, two clamping hubs and a spacer. The model selected is MIC 5, from the enterprise MAGTROL. As written in the datasheet of the element, this coupling is ready for stiff and flexible, in order to compensate axial, radial and angular misalignment, when two shaft ends are connected.

Maximun Torque	50.7	Nm
Rated Torque	36.2	Nm

Maximun speed	30000	rpm

Table 4: Mechanical characteristics of the coupling MIC 5 (Own elaboration, data obtained from MAGTROL)

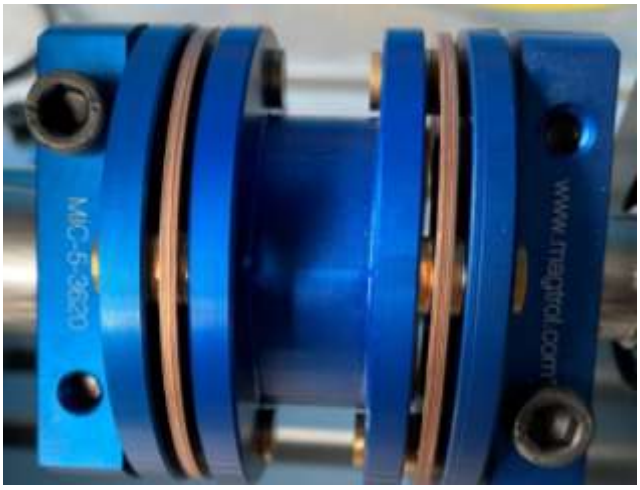

Figure 35: MIC 5 (Laboratory photo)

The other coupling presented for the connection between the torque transducer and the motor is the model GDC 80, from the enterprise called SAPIT. Some of the characteristics of this elements are presented in the Table 5.

Figure 36: GDC 80 (Laboratory photo)

Diameter	80	mm

Length	81.8	mm
ISO 4762 fixing screw	M8	-
Screw tightening torque	30	Nm
Nominal Torque	75	Nm
Torsional rigidity	20000	Nm/rad

Table 5: Mechanical characteristics of the coupling GDC 80 (Own elaboration, data obtained from SAPIT)

3.2.5. Brake and Brake Power Module

For the tests, the load applied to analyze the characteristics of the motor is going to be performed through the brake, and its current power module. The voltage selected in the LabVIEW program will be transformed into current thanks to the power module. Then this excitation current will manage the brake acting as a load to the motor.

This brake works via the principle of the hysteresis. This principle is proportional to the applied current from zero to the rated torque.

The selected model of the brake is *AHB-24,* from MAGTROL.

The characteristics of the brake are presented in the Table 6.

Minimum torque at rated current	24	[Nm]
Rated Current	2400	[mA]
Resistance ±10% at 25°C	10	[Ω]
Voltage	24	[Vdc]
Nominal power	57.6	[W]
Maximum speed	12000	[RPM]

Torque to Inertia ratio	2.140	[rad/s^2]

Table 6: Mechanical characteristics of the brake Own elaboration, data obtained from MAGTROL)

In the datasheet of MAGTROL, it is written that this brake is a highly reliable hysteresis device for tension and control torque, which induces better results for the test realized.

This is a compressed air-cooled brake, in other words when the torque measurement must be performed at the highest power, the passages of the brake enables compressed air cooling, providing excellent heat dissipation.

Figure 37

The control of the break has to be by current. For this, it is needed an element that transform the voltage into current. This action is realized by a brake power module.

The selected model is BPM103 from DSPM, recommended for easily controlling a brake.

Figure 38: Power supply to the brake (Laboratory photo)

This module is used to supply and control the current (up to 3A) of the brake previously mentioned.

Supply voltage	20 to 35	VDC
Power consumption	70	mA
Power Output Imax / Vmax	up to 3 A / UV minus 2 V	-

Table 7: Mechanical characteristics of the BPM103 (Own elaboration, data obtained from DSPM)

The electric diagram for this element is represented below:

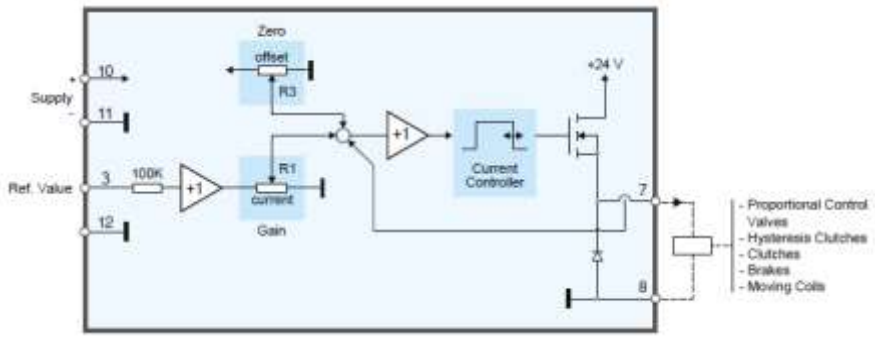

Figure 39: electric diagram of the brake Power module

3.2.6. Current Measure System

To measure the active current from the grid, meeting the needs of the motor, a current sensor will be used, that consists of two different elements, a sensor and an amplifier.

The first element, the current sensor, is from the Tektronix brand, model TCP303. This element incorporates a Hall-effect technology to provide a broad bandwidth measurement. Then thanks to the TCPA300 Amplifier, the values of the current could be amplified up to thousands of amps, because the read values of the current are low.

This Hall sensor is able to detect and measure magnetic field. It has a magnetic core to detect and analyze the flux around the wire, and address it to the Hall effect element.

The table below shows the characteristics:

Bandwidth (-3dB)	– 15	MHz
Risetime	≤23	ns
High Current Sensitivity Range	50	A/V Range
Low Current Sensitivity Range	5	A/V Range
DC Accuracy (Operating temp 0 °C to 50 °C)	±3% of reading (10 °C to 50 °C) +3%/-6% of reading (0 °C to	-
DC Accuracy, Typical (Operating temp 23 °C ±5 °C)	±1% of reading	-

Table 8: Characteristics of the current sensor TCP 303 (Own elaboration, data obtained from Tektronix)

In the analysis, the values of the current can diagnose problems such as broken rotor bars, abnormal airgap eccentricity, between others. To detect these faults and analyze the different signals in a three-phase induction motor, a system commonly known as motor current signature analysis will be used. It consists on:

- Current transformer to sense the signal (TCP303)
- A resistive shunt

In the test bench installed in the laboratory, the current transformer (TCP303) is clipped on one of the three phases of the supply cable. The fundamental reason for this, is that the rotating flux waves produced by different faults cut all three stator phase windings, and corresponding currents are induced in each of the three phases.

This will serve to analyze several current values, converted into voltage (over the resistive shunt). because the DAQ (data acquisition board, presented in 3.2.9) is capable to read only voltage values.

The illustration presented above represents the conversion:

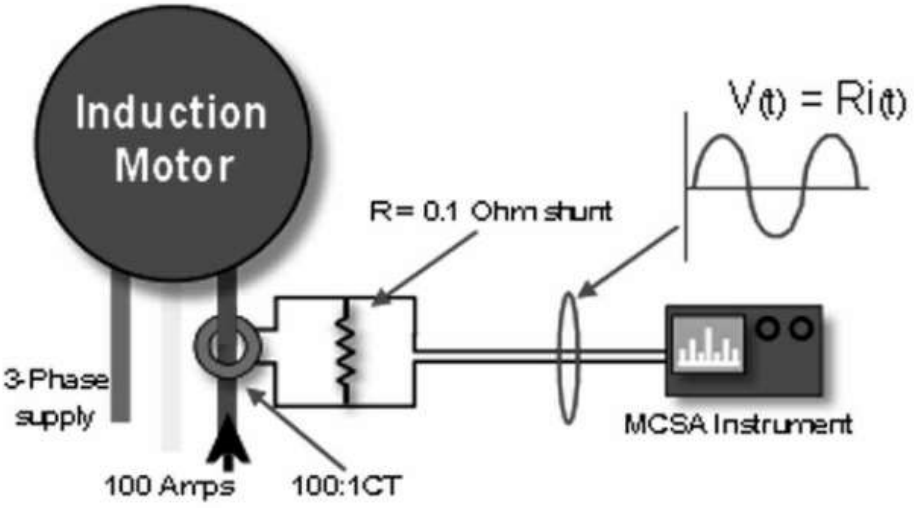

Figure 40:Instrumentation system (Thomson & Gilmore, 2003)

The transformed values from the TCPA300 amplifier represent 1V to a 5A.

Figure 41: Current measurement system (Laboratory photo)

3.2.7. Magnetic Flux Probe Emerson

The magnetic flux (represented by the Greek letter Φ), is calculated from the magnetic field.

This flux is measured on a flat surface, and it is the result of the scalar product, of the magnetic field (vector), and the vector of the evaluated area. (WIKIPEDIA, 2022)

$$\Phi = \vec{B} * \vec{S} \tag{24}$$

In the test bench, to measure the **axial flux** the sensor type M 343 F-1204, from the brand Emerson is used. This is a circular crown with an internal radius of approximately 10 cm. This core is connected to an instrumentation amplifier and a low pass filter, in order to obtain a much clearer signal.

This probe is located at the back of the motor parallel to it, in order to measure the axial magnetic flux perpendicular to the motor.

Figure 42: Emerson M 343 F – 1204, on the rear of the RAEL induction motor

3.2.8. Custom Flux Probe

To measure the **radial flux**, the probe in this case was made in the laboratory. The probe has a semicircular shape.

This is located on the top of the motor, and it has an instrumentation amplifier and a low pass filter, as the axial flux.

Figure 43: custom flux-probe for radial flux

3.2.9. Data Acquisition Board (DAQ)

The board used in the laboratory is the NI USB-6212 from National Instruments. It is covered by a plastic box for a mechanical protection.

This board serves as an interface to the PC. The main function of this board is to convert the digital signal from the computer into an analogic one, from the different elements of the bench. It can also convert from analogic into a digital signal.

It operates with a software of LabVIEW.

The parameters that characterize the DAQ, are: resolution, measurement range, gain, sampling rate and filters.

Figure 44: Data Acquisition Board (Laboratory photo)

3.2.10. Digital Wattmeter

The model of the wattmeter used is the 304B from the brand Infratek.

This wattmeter is a digital three-phase electrodynamic instrument used for measuring the electrical power or electrical energy supply rate, given to the induction motor.

It is used to measure some features like: power, voltage, current and the power factor.

Figure 45: Wattmeter (Laboratory photo)

3.2.11. Refrigeration System

When a determinate load is selected, the brake needs some refrigeration in order to not cause damage to itself. To protect it a refrigeration system is attached to the test bench.

The refrigeration system is applied to reduce the heat accumulated inside of the brake specially when a load is inserted

The model selected ESK660/100 is form the brand Compat-air, from the ultra quiet series. The type of compressor is an oil-free piston.

Figure 46: refrigeration system (Laboratory photo)

Some of the mechanical characteristics, for this compressor, working under 400V and 50 Hz conditions, are:

Power	3.20	kW
speed	1400	rpm
Nominal current	6.5	A
Max Pressure	10	bar
Performed sound	76	dB

Table 9: Characteristics of the model ESK660/100 (Own elaboration, data obtained from Compact-air)

4. ANALYSIS FROM THE GRAPHS

In this chapter, the results given by the test bench will be analyzed and studied in detail, with the purpose to understand the different signals given by the motor, and comprehend how it works.

For the tests, the load applied to analyze the characteristics of the motor is going to be performed through the brake, and its current power module. The voltage selected in the LabVIEW program will be transformed into current thanks to the power module. Then this excitation current will manage the brake acting as a load to the motor.

To achieve this, different voltages will be selected thought the LabVIEW software, in order to change the different load values applied to the test bench, and understand how the motor reacts to these different values.

The values of the test, are allocated in the stable region of the motoring region (2.2). This means a variation in the voltage from 0V, which means no load, until 4V, the value to reach the nominal torque, the optimal value to work.

Note: The analytic values, through which these graphs have been obtained, can be seen in the data table of the annex (7.1).

4.1.Torque-speed & Rotor Speed-Voltage

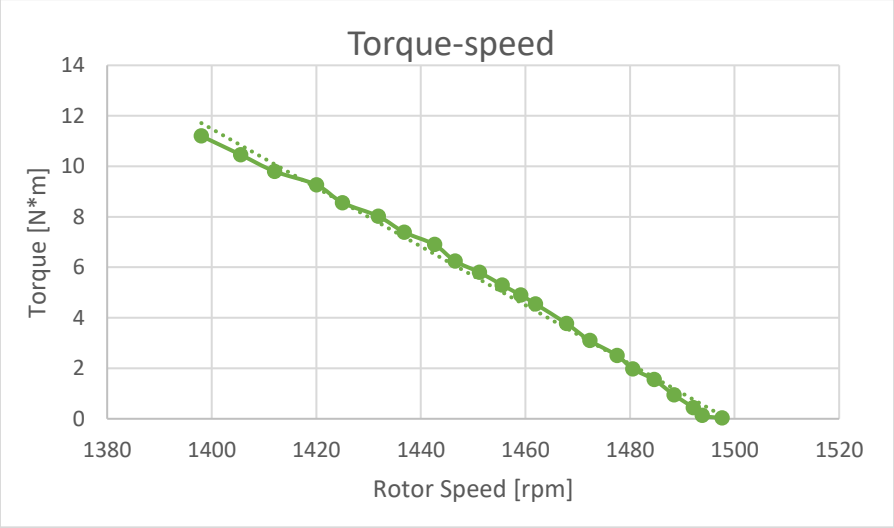

Figure 47: graph Torque-rotor speed

The first graph studied is the *Torque-Rotor Speed* curve. It shows part of the working zone of the motor. It is located in the stable zone, following a linear comportment, from 0 Nm until 10.4 Nm.

When the value of the torque is close to zero (it has a little value of 0.029), it means that no load is applied, as explained in the graph of Torque-voltage**,** so the selected voltage is 0 volts. In this condition the speed reached by the rotor with the value of 1497.6 rpm takes is maximum, close to the synchronism speed (1500 rpm).

If the speed of the rotor were the same as the synchronous one, the relative speed would be zero, and this would imply that the magnetic flux in the bars would be null. Therefore, there would be no electromagnet force and no torque. This is also the reason, why the value of the torque is not null.

When the torque experiments an increment, this means that a load is applied, and the value of the rotor speed suffers a decrease. The decrease in the speed is directly related with its frequency, and the relation between them.

$$f_1 = f_2 + f_r \tag{25}$$

When the speed of the rotor decreases, the value of the frequency of the rotor currents will increase (f_2); therefore, the value of the frequency of the movement of the rotor (f_r) decrease, because f_1 has a constant value of 50 Hz, and the values of the other two frequencies change according to this relation.

Also, this relation can be explained through the formula:

$$P = T \times \omega \tag{26}$$

The formula (*26*), represents the relation between the output power of the motor (P), the measured torque (T), and the angular speed (w).

The output power of the motor is greater when the load increases, and the value of the angular speed of the rotor will suffer a little decrease.

A similar analysis could be done, between *Rotor Speed-Voltage*, because the voltage values and the torque ones are directly related.

As can be seen in the Figure 48, the mechanical speed of the rotor (n) decreases as the input voltage to the brake increases, due to the fact that the load has risen, the speed reached by the rotor is going to be decreased; this means higher load, lower speed.

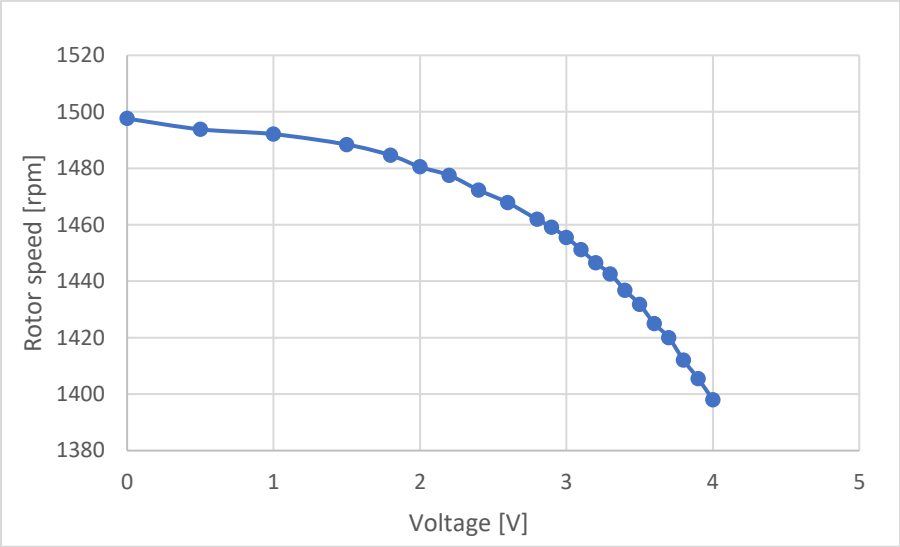

Figure 48:graph Rotor speed-voltage

4.2.Torque-silp

In this graph, the relation between *Torque-Slip* is represented. When the torque gets higher values, this means that the load applied is bigger (the input voltage selected is greater), so the speed of the rotor will decrease.

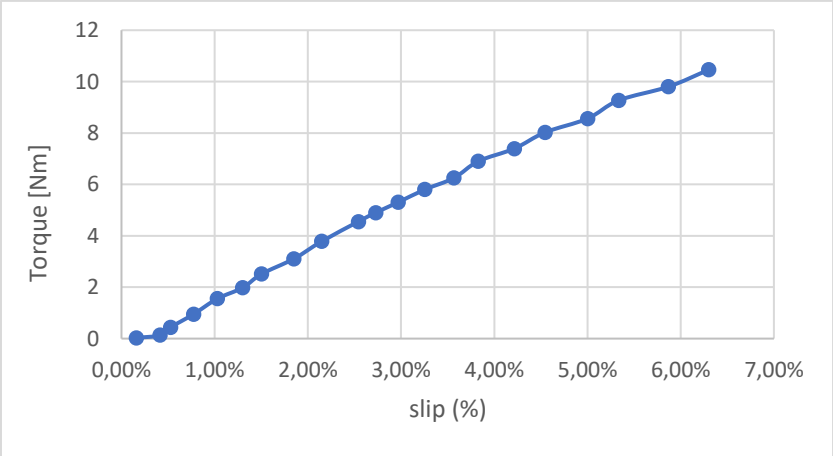

Figure 49:graph torque-slip

For the formula:

$$s = \frac{n_1 - n}{n_1} \tag{27}$$

n_1 is the speed of synchronism (in this case 1500 rpm), and n the speed of the rotor. This slip represents the relative difference between the speed of the stator magnetic field (synchronous speed) and the mechanical speed of the rotor.

In the Figure 49, when the value of the slip is close to zero, the rotor is rotating at a speed near to the synchronism one, resulting small values for torque. On the contrary, the higher values reference to the case when a load is applied, the speed of the rotor is slower, and the slip takes higher values.

When no load is applied, the value of the silp is 0.16%, and the speed if the rotor is no 1500 rpm. This is due to some friction, ventilation and Joule effect losses in the stator.

The value of the slip is normally measured in percentage. This percentage gets bigger as the speed of the rotor decreases.

As a conclusion, the values of the slip and torque are directly related, because when the value of the torque changes, the slip does in the same way.

4.3.Torque-voltage

As explained in the previous graphs, the value of the torque is directly related with the voltage applied to the brake. In this section, this relationship will be explained.

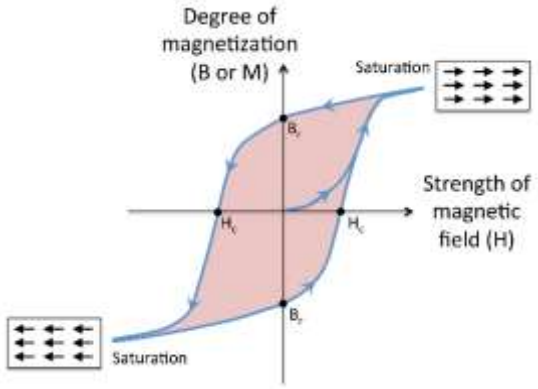

Figure 50: Principle of the loop (WIKIBOOKS, 2022)

In the graph below (Figure 51), the values for *voltage-torque* are represented, where the hysteresis due to the phenomenon of the magnetic reluctance can be studied. The hysteresis referrers to a delayed response, to a stimulus that has been applied; for example, a magnetic field with delayed magnetization or flux density.

This hysteresis loop gives information about the magnetic properties of the brake. In the case below the relation between the torque and the voltage introduced is presented.

The curve reported in this Figure 51 represents the principle of the loop, made by the hysteresis, corresponding to the first parabolic performed in the start-up. However, the values obtained from the tests are not enough to reach the first saturation of the magnetization.

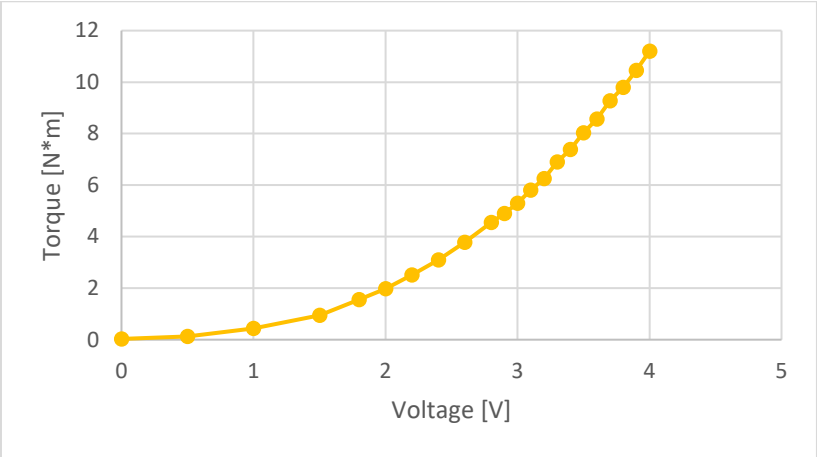

Figure 51: graph Torque-Voltage

5. LABORATORY TESTING AND SIGNAL ANALYSIS

5.1.Introduction

In this chapter will be analyzed the results taken from different experiments realized on the test bench. These experiments are made with a completely healthy motor.

The results are going to be analyzed mainly on the MATLAB program of MathWorks company. Conversely, the measurements are carried out through the use of the National Instruments Digital Acquisition Board (DAQ), model NI-USB6212, controlled by a personal computer via the LabVIEW software.

The occasion of these experiments is to understand the behavior of a healthy motor, and to study the signals related to it. Moreover, a comparison between the various physical signals acquired will be presented.

To acquire the most information from the signals, a frequency-domain analysis is carried out. However, both time-domain and frequency-domain graphs will be presented in the study to have a more comprehensive view of the physical aspects of the machine. The comprehension of some points will be held by the explanation of the phenomena known as Broken Rotor Bars further explained in detail.

Thought the machine analyzed is healthy, particular attention will be paid to the search for the signatures of the broken rotor bars, a fault known from literature, that is relatively easily recognizable with diagnostic techniques, e.g. with the Motor Current Signature Analysis (MCSA) technique. (Thomson & Gilmore, 2003)

The fault will be explained in the following paragraphs. Successively a deep analysis of the signals will be presented, focusing where special points related to this phenomenon can be.Phenomenon of rotor bar breaking

This phenomenon causes the failure explained in the chapter 2.4.3.

First, the concept of slip frequency will be introduced. Knowing that f_1 represents the supply frequency of the currents of the stator, and f_2 represents the slip frequency of rotor currents in Hz, the relation between both frequencies is:

$$f_2 = s\, f_1 \tag{28}$$

Also, the frequency of the mechanical rotation of the rotor is $f_m = (f_1 - f_2)/pp$, being pp the pole pairs of the machine; in the case of study pp is equal to 2.

In the case of a **symmetric rotor**, where there is no damage or broken bars, what the stator sees in a relative position, the result of the currents (f_2), and the mechanical

frequency of rotation multiplied by the number of pole pairs (f_r). The sum of the two frequencies makes the result as:

$$sf_1 + f_r \text{ pp} = sf_1 + (1\text{-}s)f_1 = f_1 \quad (29)$$

There are no relative differences between the stator and the rotor fields speed, seen from the stator.

In the case of the **bar breaking**, from a stationary point of view to it, can be seen the relative difference that exists between these two frequencies, the rotor currents in a cage winding producing an effective three-phase magnetic field, which has the same number of poles as the stator field, rotating at slip frequency (f_2) with respect to the rotating rotor (f_r).

This phenomenon starts with a rotor asymmetry, producing a backward rotor rotating field at a frequency of $-sf_1/pp$ (being f_1 the frequency of the currents of the stator, divided by the pole pairs), and a rotor current component frequency $-sf_1$. What the stator sees is a backward rotor rotating field at frequency: $-sf_1 + (1-s)f_1 = (1\text{-}2s)f_1$

The backward rotating rotor field induces an electromotive force in the stator, resulting a stator current peak at $(1\text{-}2s)f_1$. Also it produces another stator current peak at $(1+2s)f_1$, due to the speed oscillation generated by the non-uniform rotating rotor field. Thus, there will appear two lateral peaks (sidebands) due to amplitude modulation of a central frequency (that can be the supply frequency or its multiples) resulting in a left and a right sideband.

According *to* (Thomson & Gilmore, 2003)*"a magnitude difference of less than 26 dB between the supply harmonics and the sidebands from a one-off measurement, equates to a serious broken rotor bar problem"*. According to this, an amplitude difference between the peaks higher than 26 dB, indicates a healthy motor. Note that it is absolutely normal to see the sidebands around the supply frequency at $\pm 2sf_1$, but they indicate a broken rotor bars problem only if the sidebands surpass this difference threshold of 26 dB, according to (Thomson & Gilmore, 2003)

5.3.Analysis

To analyze, study and understand the different signals given by the motor from the test bench located in the laboratory of diagnostics of electrical machines, at University of

Pavia, different tests have been realized with a healthy motor exposed to disparate conditions.

The different data from these tests have been acquired thanks to the program LabVIEW, but transferred later in MATLAB, to survey the different important diagnostic features from the graphics extrapolated with program scripts.

Into the MATLAB code, some parameters are shaped and adjusted in order to meet different important points that can be useful for study. Also, they are adjusted according to acquire (with an adequate resolution), all the signals coming from the different sensors, that form the test bench.

Some important characteristics and parameters of the code are:

- Number of sample points for each measurement: 2^{19}. It has been chosen a number equal to a power of two because it optimizes the transformations in frequency domain.
- Sample frequency: 20 kHz

Note: The Nyquist frequency is half the sample frequency, so, in this case, the signal can be reconstructed in frequency domain till a bandwidth of 10 kHz, retained enough for diagnostic purposes in mains-fed machines. Since most of the signals analyzed (the current and the stray flux signals) has an antialiasing low-pass filter, with cut-off frequency of 2 kHz, into their amplification chain, a minimum sample frequency of 4 kSample/s (the double the bandwidth of the signal) should be selected to avoid the aliasing phenomenon. However, following a common rule used in practice, it has been chosen to sample the signal with a frequency 10 time the original bandwidth. So, being the bandwidth of the signal limited by the antialiasing filter at 2 kHz, the 20 kSample/s sampling frequency has been selected.

With this information the acquisition time results:

$$T = \frac{number\ of\ sample\ points}{sampling\ frequency} = \frac{2^{19} sample}{20\ {Ksample}/{s}} = 26{,}214\ s \qquad (30)$$

Then, each sample segment is about 26 s. To successively perform a mean of the data, a set of 20 segments is taken for each condition of the machine.

The frequency resolution achievable in a Discrete Fourier Transform (DFT) is the inverse of the sample time, so in this case it results:

$$res_{DFT} = \frac{1}{T} = \frac{1}{26.214} \approx 0.0381\ Hz \tag{31}$$

To be noted that for the frequency domain transformation of the data, the MATLAB function *pspectrum* has been used*;* this function allows to choose the desired frequency resolution in order to save computational time and resources. However, the resolution chosen in the function must be higher than the resolution calculated by the formula above (*31*), that represents the minimum resolution achievable in the frequency transform.

In any case, the results provided by the MATLAB code are presented in two different domains. The first one is the **time-domain**, were the signals measured in voltage are presented (the conversion scale to calculate the values of the current in amperes is 5 A/V, (3.2.5 paragraph). The second one is the **frequency domain**, obtained thanks to the Fourier transformation (as previously mentioned, the *pspectrum* MATLAB function has been used for the transformation).

These tests are carried out with a completely healthy motor, model RAEL 90 L 4, with a synchronous speed of 1500 rpm, and other characteristics exposed in 3.2.1.

The supply frequency, or the frequency of the currents of the stator, has a value of 50Hz, since the motor has been supplied by the main grid.

5.3.1. First Test: No Load

This first test is performed without any load, so no excitation current is given to the magnetic hysteresis brake, what means that no control voltage has impressed into the BPM 103 current supplier.

The results obtained from the LabView software related to this first test are:

- Torque induced: 0 Nm (no excitation current is applied)
- Speed of the rotor: 1494 rpm (close to the synchronous speed)

In this test, because there was no load, the torque is null, making the speed very similar to the synchronous speed; but as said before, this speed will be never reached, due to the fact that if the speeds are the same, the electromotive force induced in the rotor circuits will be zero, making no current flowing through the bars, and no electromagnetic forces available to win the mechanical losses of friction and windage.

From the speed value in *rpm*, the value of the frequency of the rotor speed can be calculated, through this formula:

$$n_m = \frac{60 \times f_r}{pp} \tag{32}$$

Where n_m is the mechanical speed of the rotor in *rpm* (that assume the value of 1494rpm), and the parameter f_r is the frequency of the electrical quantities seen from the stator (f_r corresponds to the mechanical frequency of rotation multiplied by the number of pole pairs).

Clearing the formula in order to obtain the stator electrical frequency variable, it results:

$$f_r = \frac{1494 \times 2}{60} = 49.8Hz \tag{33}$$

With this frequency, the value of the frequency of the rotor currents (f_2) is calculated as follows:

$$f_2 = (f_1 - f_r) = 0.2Hz \tag{34}$$

Then, to calculate the frequency of the speed of the rotor, f_r is divided by the number of pole pairs (two, in the case analyzed):

$$f_m = \frac{f_r}{pp} = \frac{49.8}{2} = 24.9Hz \tag{35}$$

Finally, to obtain the value of the slip, the formula used is:

$$s = \frac{n_1 - n}{n_1} = \frac{1500 - 1494}{1500} = 0.004 \tag{36}$$

So, the results are:

- Frequency of the rotor: 24.9 Hz
- Frequency of the rotor currents: 0.2 Hz

Also, there are some other results directly given from the wattmeter:

Motor's stator phase	Absorbed power	Absorbed current

Phase 1	67.32 W	2.69 A
Phase 2	101.35 W	2.80 A
Phase 3	95.58 W	2.57 A
Power Factor =0.10		

Table 10: wattmeter no-load

5.3.1.1. Time Domain analysis

In the Figure 52, the signals are presented in the time domain. They are measured in a scale of voltage.

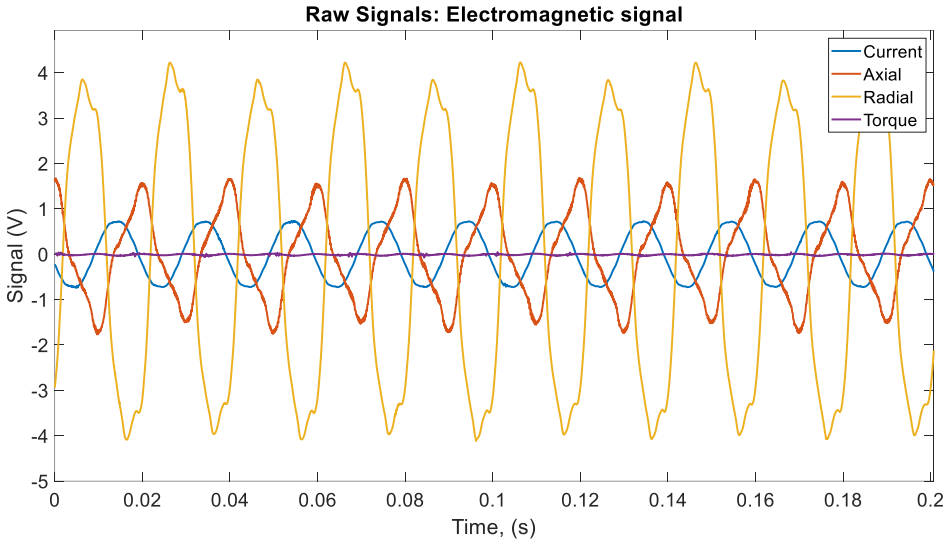

Figure 52: Time domain no-load

Taking a look at the **current** signal (depicted in light blue in the figure), it can be seen that the values reached go from -0.725V to 0.704V peak to peak (to convert the signal in amperes it has to be multiplied by the 5 A/V selected range of the current transducer, which leads to a current value reasonable for the motor). This current waveform looks like a sinusoidal wave; this is because the machine is fed directly from the grid. However, the waveform is not perfectly sinusoidal; in fact, as can be noted performing a harmonic analysis, many harmonics are present in the spectrum other than the fundamental one, especially the odd multiples of the fundamental harmonic. Moreover, it has to be remembered that the stator current in an induction motor is more distorted in no-load conditions, since the magnetizing current component is higher with respect to the load current, and the former is often distorted due to the nonlinear B-H curve of the material.

The **torque** signal represented should be zero, as no excitation current is applied to the brake. However, it can be noticed some torque ripples at 100 Hz; these ripples could be generated due to the construction imperfection of the motor. It is interesting to notice that it has been possible to measure these torque ripples thanks to the inertia given by the brake that counteracts the motor torque variations (the torque transducer reads a difference of torque between the two connected shafts).

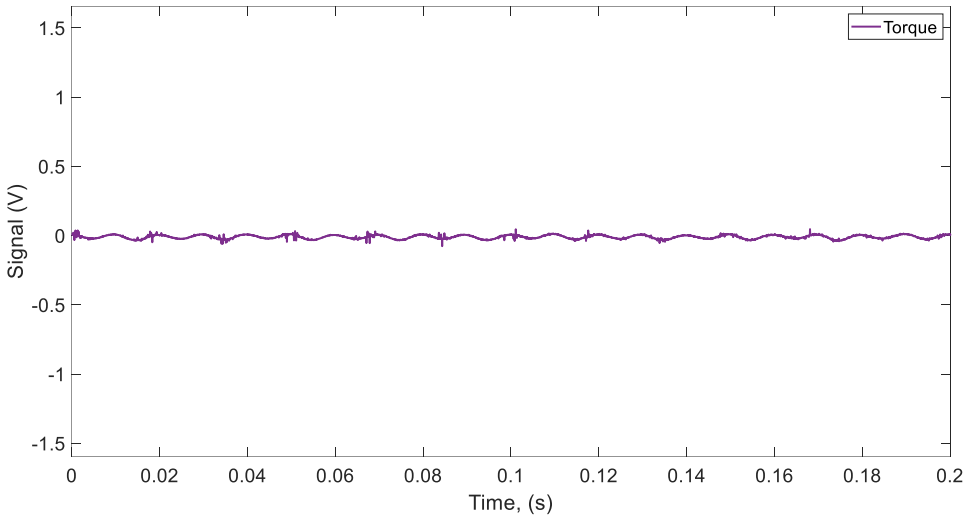

Figure 53: Time Domain no-load Torque

The **flux** signals, as can be seen from the time domain figure, contain many harmonics, and are very different from a sinusoidal waveform. As can be noted looking at the following graphs in the frequency domain, the harmonic magnitudes of the flux signals will be higher than that the current signal, by comparing the magnitude of the fundamental with the higher order harmonics.

5.3.1.2. Frequency Domain analysis

A representation in the frequency domain of the current, stray fluxes and torque signals is presented in the next figure.

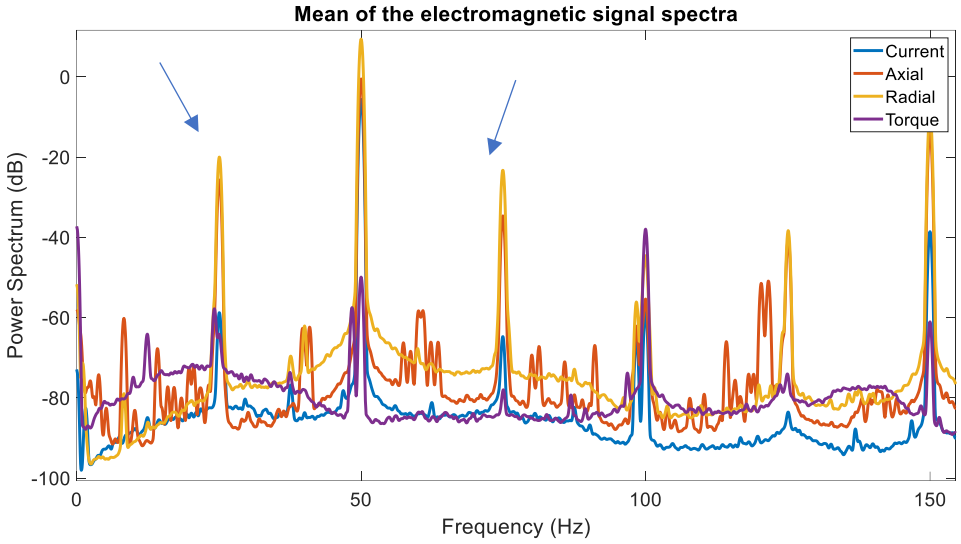

Figure 54: Frequency domain no-load

Observing the signals shown in the Figure 54, by a first look it can be seen that the harmonic at 50 Hz is the most pronounced. This is a direct consequence of the frequency of the grid, that is 50 Hz, so all the components close to it should be higher.

Also, are pronounced the higher order harmonics at multiples of 50 Hz, that are 100Hz, 150Hz and so on.

Looking at the graph, it should be noted that the even harmonics are less accentuated than the odd ones, especially for the current signal. The even harmonics are normally very low in amplitude thanks to the anti-symmetry of the two semi periods of the current signal: shifting the signal by half period in time, the following semi-period is equal to the first one. Due to this property of the signal, the Fourier transform give rise to a spectrum in which all the even harmonics are ideally null (in practice, they have some amplitudes because the signal is not ideal).

The **flux signals** are the richest in harmonics, also noted in the time domain, in which the waveforms are very different with respect to a sinusoidal wave (they are deformed due to the numerous harmonics). So, as commented before, the waveforms are composed by a lot of harmonics that can be evaluated in a more punctual way in the frequency domain. The reason of such deformation of the flux signals can be found in the complicated physics behind them: the fluxes are shielded by the frame of the motor and they are composed by various components due to stator currents, rotor currents, and end-windings or ring currents in the rotor. The values of the flux signals represented in the frequency domain can give information also to detect faults, or evaluate the state of the motor; and in some cases, they outperform the current signal, since studies in literatures demonstrate their sensitivity for some faults, e.g. bearing faults.

Other important peaks can be found around each of the odd harmonics of the electromagnetic signals, in the form of sidebands. These sidebands are at frequency given by the formula:

$$f_{side} = k \cdot f_{supply} \pm f_m \tag{37}$$

These harmonics, though often recognized as eccentricity harmonics, when surpass a certain threshold can be ascribed to an axes misalignment defect, according to Thomson. These sidebands are highlighted with arrows in the previous image, for clarity. (Thomson & Culbert, Current Signature Analysis for Condition Monitoring of Cage Induction Motors: Industrial Application and Case Histories)

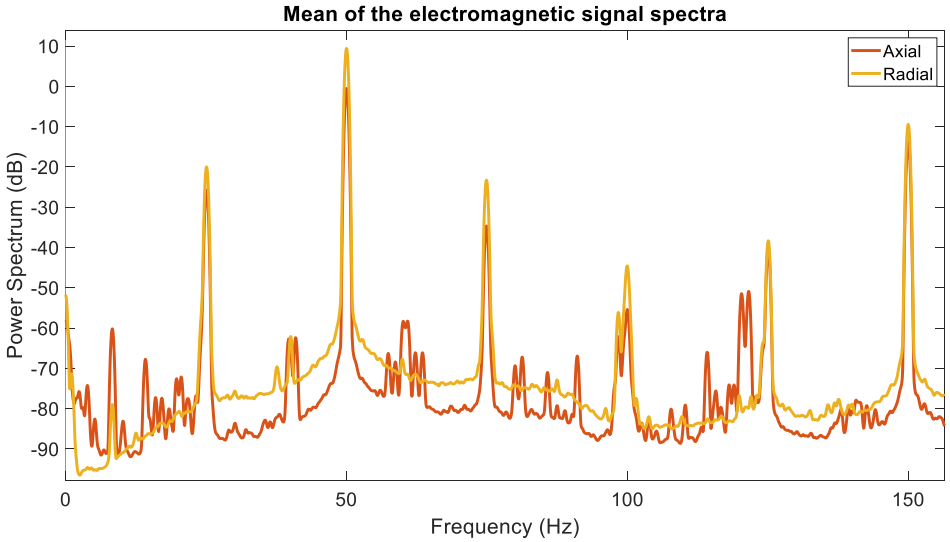

Figure 55: Frequency Domain no-load flux

In this graph, both values of the **fluxes** are compared, and it can be seen that they take similar values, but the axial one experiments more harmonics that interfere and modify the value of the signal the time domain. In the case of the axial flux, more harmonics can be seen that in the radial flux, probably because it collects the magnetic field from the end windings of the machine; the radial flux should be more similar to the airgap flux, i, e. more sinusoidal.

As explained previously, in the graph in the time domain, the measured **torque** had some ripples at 100Hz, due to the construction imperfection of the motor. In the Figure 56 is showed above a peak at that frequency can be noticed.

As Yasser Gritli says in his article," this can be caused by some stator asymmetry of the machine that forms a reverse rotating magnetic field. Due to the stator asymmetry, the currents flowing through it, are not symmetrical, inducing a counter rotating field at twice

of the supply frequency". The counter-rotating field induces a pulsating torque and a speed oscillation at frequency 2f. (Gritli, 2014)

At last, it can be noted that the torque spectrum has a peak in 0 Hz, that means that is working under continuous torque conditions, and no oscillation is applied to it. However, it can be noted that the magnitude of this peak is low (-37.3 dB), and in fact no constant torque has been applied to the motor by the brake (it is a no-load condition). The following graph represent the torque signal and its major peaks for the no-load condition in a frequency range from 0 to 150 Hz.

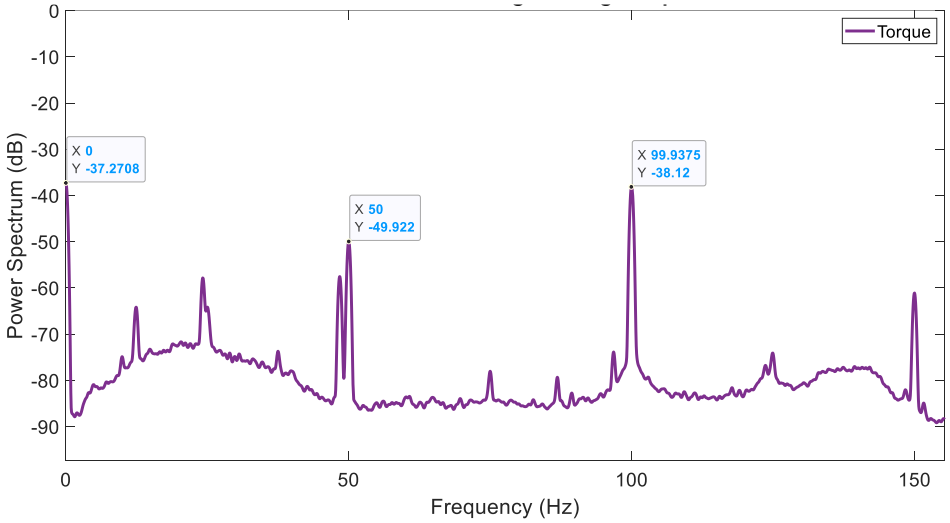

Figure 56: Frequency Domain no-load torque

Additionally, the graphs of **the current and the torque** are closely related one each other; giving similar values. This can be easily explained by the following formula of the torque.

This formula is related to the power given from the stator to the rotor. This torque is the result of the ratio between P_u, named as the useful power (2.6), and the angular speed of the rotor.

$$T = \frac{P_u}{2\pi \frac{n}{60}} \tag{38}$$

If the losses of the rotor are not taken on account, the formula used is:

$$T = \frac{P_{mi}}{2\pi \frac{n}{60}} \tag{39}$$

Where P_{mi} represents the mechanical power (2.6).

Following the Figure 57 represented above the mechanical power can be represented as:

$$P_{mi} = m_1 R'_2 (\frac{1}{s} - 1) I'^2_2 \quad (40)$$

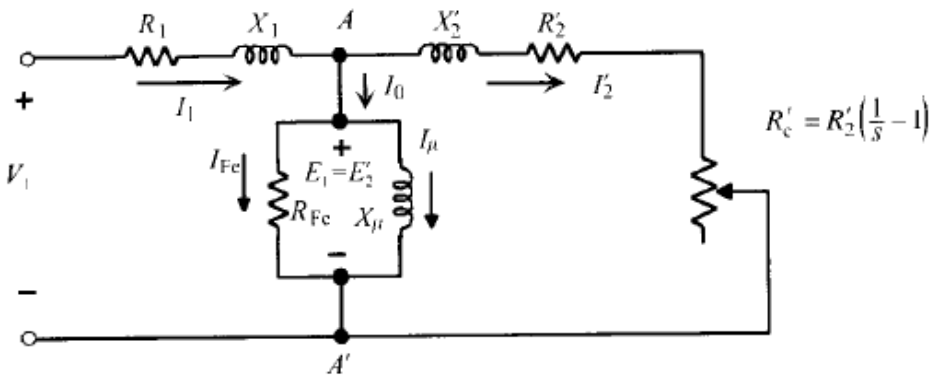

Figure 57: scheme of an induction motor (Fraile Mora, 2003)

Also, the relation between the currents, deduced from the scheme, is:

$$I_1 = I_0 + I'_2 \quad (41)$$

Whether an increment in the current from the grid exists, the current passing through the rotor increases more or less in the same way (because the current I_0 is small). Also, knowing that the mechanical torque has a direct relation with the current, when the current experiments an increase the power does, resulting an increase in the torque.

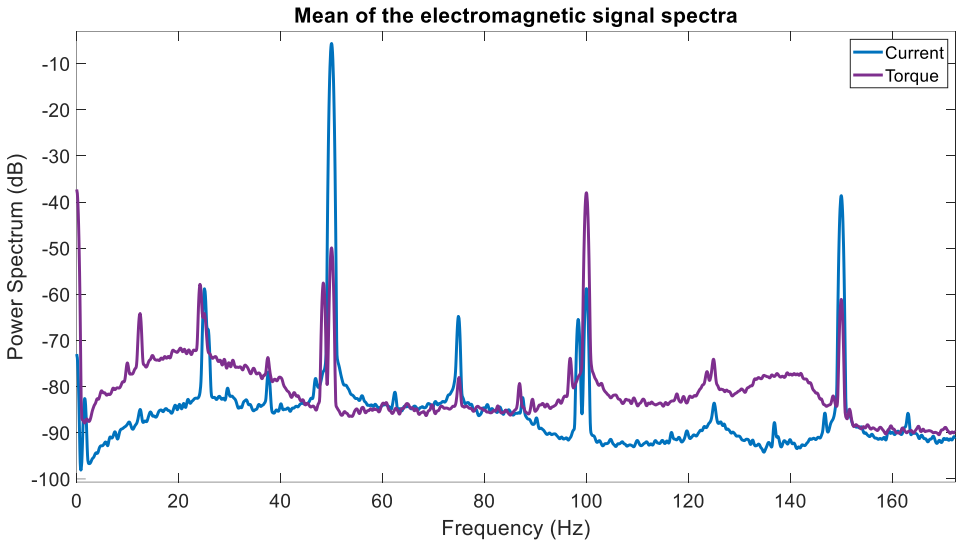

Figure 58: Frequency domain no-load torque and current

Broken Rotor Bars analysis

In this case, as previously shown, the value of the frequency of the currents of the rotor (f_2), is really low, and the slip takes the value 0.004, which means that both speeds are really close one to each other.

To evaluate the possible points of the broken rotor bars, in the graph of the current, the points calculated with the formula are: (formula shown in 5.2)

- f_1= 50Hz
- left frequency= 50(1-2*0.04) = 49.6 Hz
- right frequency= 50(1+2*0.04) = 50.4 Hz

In the figure below the graph of the **current** in the frequency domain is represented. It can be seen that there is a remarkable peak in the supply frequency (50Hz) reaching a value of -5.63dB, but there are no lateral peaks referred those for detecting the broken rotor bars. This is caused by the low value of the slip (the lateral peaks tend to merge with the central one) and to the low value of the current in the rotor in no-load condition.

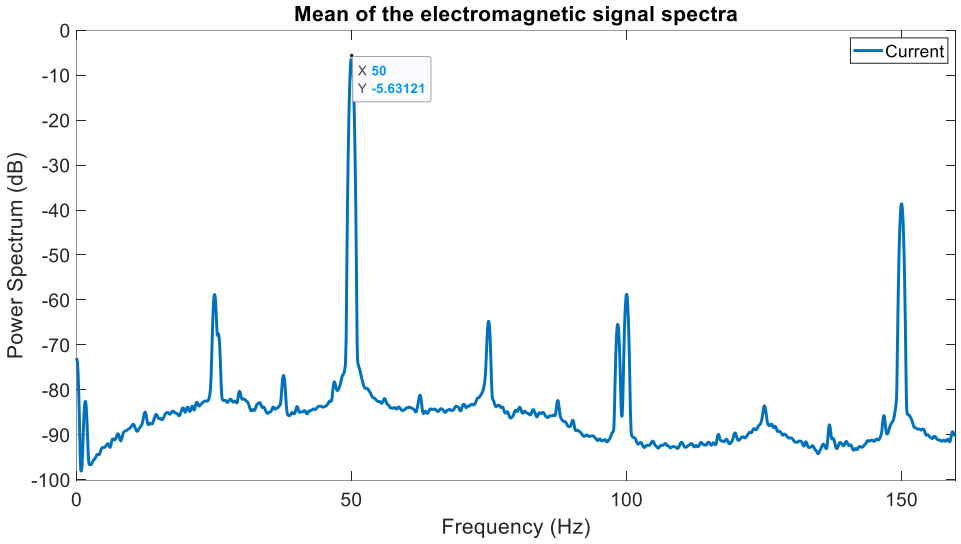

Figure 59: Frequency Domain no-load current

	Frequency [Hz]	Magnitude [dB]
Supply frequency	50	-5.63
Left sideband	49.6	-
Right sideband	50.4	-

Table 11: Current no-load values for Broken Rotor Bars

Conversely to the current signal in which there are some thresholds to consider to distinguish the faulty with the healthy case (the motor does not have broken rotor bar, if the magnitude difference between the central peak and the lateral peaks is more than 26 dB according to Thomson), with the **flux signals** it is difficult to stabilize effective threshold, since the intensity of the signal can vary a lot with a little displacement of the flux probe.

Taking a look to the **radial flux**, the peak should be located at the same frequencies than the current, so as happened with the current, these peaks cannot be noticed, due to the low slip of the motor and the low rotor-current.

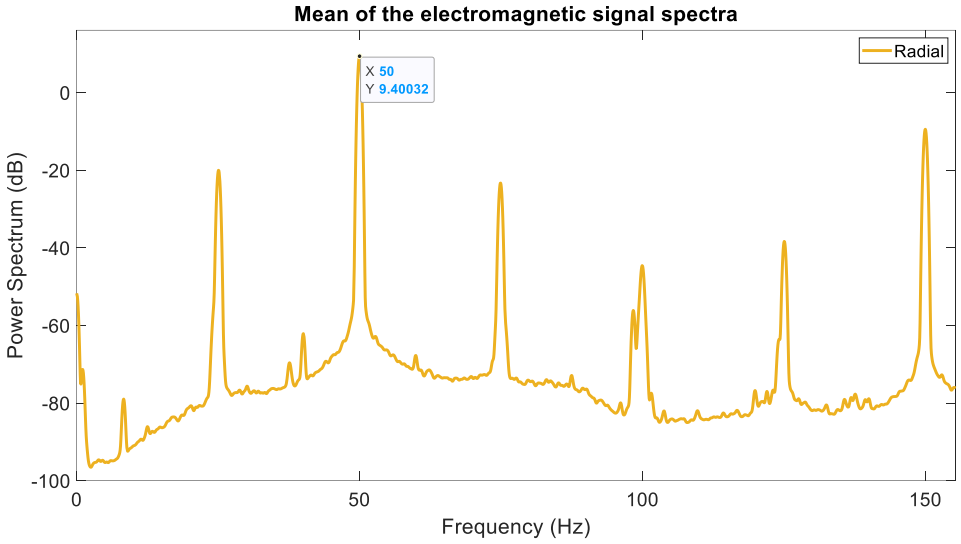

Figure 60: Frequency Domain no-load Radial flux

	Frequency [Hz]	Magnitude [dB]
Supply frequency	50	9.40
Left sideband	49.6	-
Right sideband	50.4	-

Table 12: Radial flux no-load values for Broken Rotor Bars

In the case of the **axial flux**, the result obtained is the same as for the radial flux; the sidebands peaks cannot be noticed.

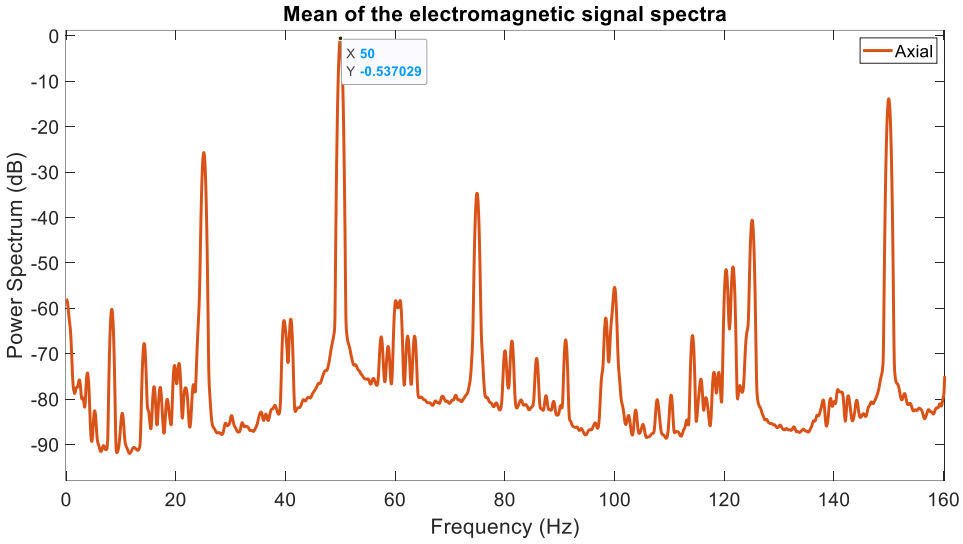

Figure 61: Frequency Domain no-load Axial flux

	Frequency [Hz]	Magnitude [dB]
Supply frequency	50	-0.53
Left sideband	49.6	-
Right sideband	50.4	-

Table 13: Axial flux no-load values for Broken Rotor Bars

5.3.2. Second Test: Constant Load

This second test, has been realized in the same conditions as the first test, but experimenting a change in the mechanical load applied (through the brake 3.2.5). The load set in the experiment is constant, with approximately an 80% of the rated load, that is a torque value that can be applied to the motor continuously, without having an abnormal overheating of the machine.

Since a load is applied to the motor through the brake, there would be some dissipation turned into heat, due to the torque applied by the brake. The power dissipated can be calculated multiplying the braking torque in [Nm] by the rotational speed in [rad/s]. For this reason, the refrigeration system should be in operation, in order to not damage, due to overheating, the brake. The cooling system consists of a bundle of compressed air injected into the stator of the brake; the air passes over both the stator and the rotor to

extract heat. To compress the air, a compressor with a considerable air flow rate described in paragraph 3.2.5 is used.

The control voltage introduced into the BPM 103, the current supplier of the brake, is constant, with a constant value of 3.5V, in order to create the desired constant load.

The read values from the software of the torque transducer are:

- 1430 rpm (rotor speed)
- 8,42 Nm (the value of the read torque)
- 1242 W (braking power, that corresponds to the mechanical output power of the motor)

The value of the speed, with respect to the previous test performed, has decreased, since the torque has now a higher value, and the machine is not controlled in speed. As explained in the chapter 4.3, when the torque gets higher values, because it increments as the load does, the speed of the machine becomes lower, moving away from the value of the synchronism speed, since the slip is increasing its value.

The values of the slip or those of the frequency, are obtained with the same formulas presented in the previous test.

The obtained values are:

- f_1= Supply frequency, or frequency of the stator: 50Hz
- f_2= Slip frequency, frequency of the current of the rotor bars: 2.4Hz
- f_m= Frequency of the rotor speed 23.8 Hz
- s= Value of the slip 0.0467

The results of the wattmeter were:

Motor's stator phase	Absorbed power	Absorbed current
Phase 1	520.47W	3.35 A
Phase 2	564.50 W	3.507 A
Phase 3	553.53 W	3.321 A

Power Factor =0.687

Table 14: wattmeter constant-load

The read values show higher absorbed power and current, from the no-load test as could be expected.

Moreover, it can be noted that the power factor is increased as well, reaching a value of 0.687 (with respect to the no-load case in which it was 0.10); this is expected in induction motors where from a no-load condition to a loaded one, the current increases but not as much as the absorbed power does, due to the simultaneous increase of the power factor in the following formula:

$$P_{abs} = \sqrt{3}\, V_{line} I_{line} \cdot \cos\varphi \tag{42}$$

Where V_{line} and I_{line} are the line voltage and line current of the three-phase motor, $\cos\varphi$ is the power factor and P_{abs} is the electrical power absorbed by the motor. More explained in chapter 2.7

5.3.2.1. Time Domain analysis

In the time-based graph (visible in the next figure), the first thing that can be noticed is that the mean value in voltage of the **torque** signal is not zero, because some excitation current is applied to the brake, giving a final value of the torque signal of around 2 Volts. As in the previous case some ripples are present at 100 Hz, and some spikes are present probably due to some disturbances in the measurement.

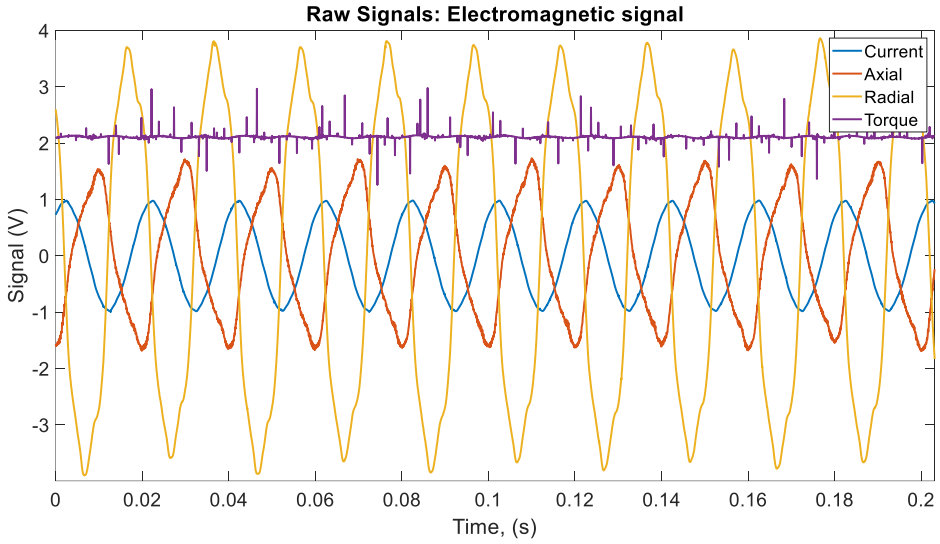

Figure 62: Time domain constant-load

The **current** signal reaches higher amplitude values, as expected confronting the values of the wattmeter readings from the no-load and constant-load conditions. The values of the current signal go from -0.96 V to 0.96V, peak to peak.

Since the requirement of input power from the motor is higher, because a load is applied, the active current required from the grid increments. This is the reason why an increment of the values of the current can be noted.

As regards the **flux** signals, it is difficult to notice any difference between load and no-load condition in the time domain: the amplitude of the signal remains more or less the same in the two conditions; the only thing that can be noted is that the radial flux signal is more smoothed in its shape in the load-condition, than in the no-load condition.

5.3.2.2. Frequency Domain analysis

The frequency spectra of the signals for the constant-load condition are represented in the next image.

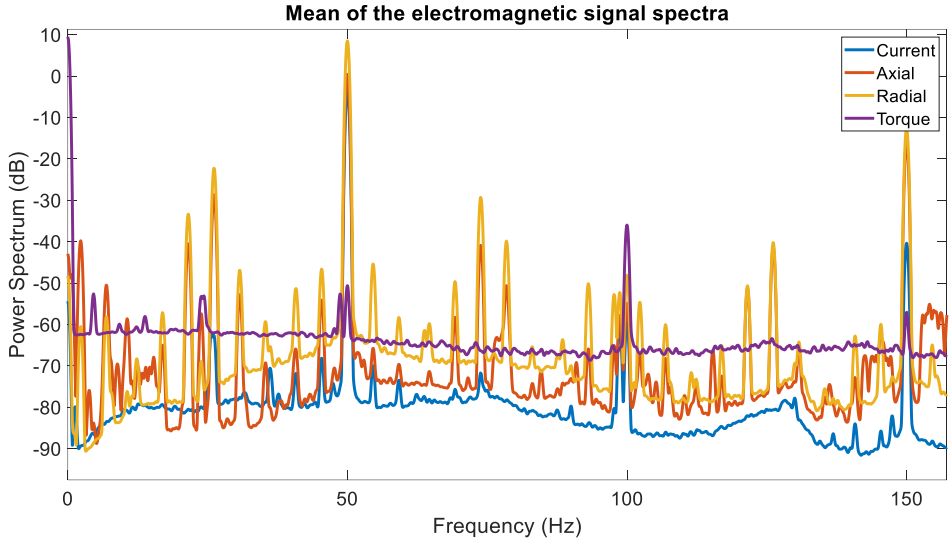

Figure 63: Frequency domain constant-load

At a first look to the graph, it can be noted a higher quantity of harmonics with respect to the graph of the no-load condition.

Starting with the **torque** signal, first of all it can be noticed that it presents a peak at the frequency of 100Hz; the explanation to this phenomenon could be the same given as in the no-load condition: the torque ripples should be present because of the intrinsic asymmetries in the machine due to construction imperfections. Moreover, it can be noted a peak in 0 Hz, indicating that there is a mean value of the torque different from

zero Nm (constant torque) between the motor and the brake; so, the motor, is working under constant load and torque condition.

In terms of magnitude, the value of the torque at the zero Hertz in frequency, reaches a higher peak, even above zero decibel, than that detected in the no-load test. In the first test, the value in decibels of the torque takes a negative value, not even close to zero, around - 40dB. As expected, when a higher load is applied, the value of the torque increments, and is reflected in the value of the peak in the torque.

The values of the **current** harmonic peaks, seen in the frequency domain**,** are generally higher than that of the no-load case as expected, since the value of the current increases. For the current the maximun peak is experimented at 50 Hz, wich is the supply frequency. Other important frequencies are its multiples, at 100 Hz and, as seen in the figure 150 Hz, that are its first two harmonics.

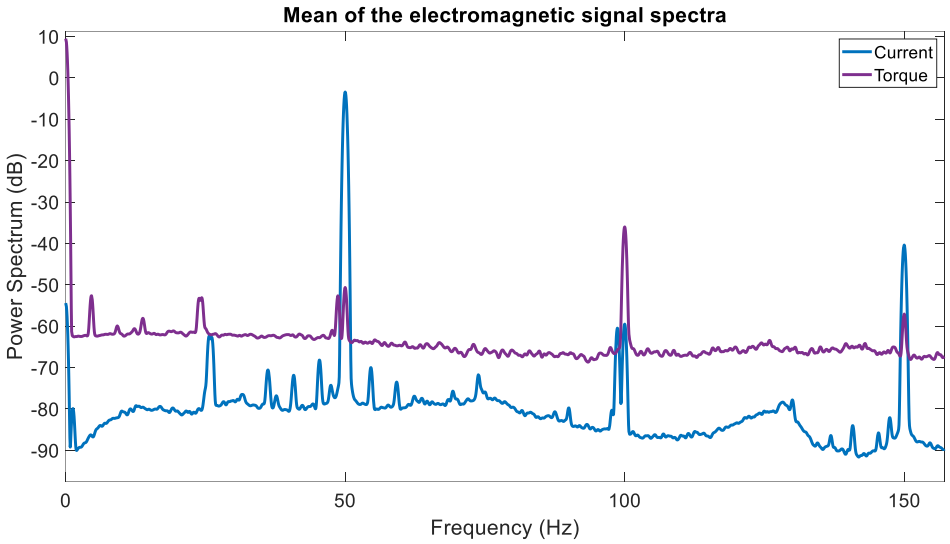

Figure 64: Frequency domain constant-load Current Torque

Broken Rotor Bars analysis

Taking the value of the slip, previously calculated, equal to of 0.0467, and calculating where the different sidepeaks should be placed in the frequency domain, for the examination of this penomenon, the presented values are:

- f_1= 50Hz
- left frequency= 50(1-2*0.0467) = 45.33 Hz
- right frequency= 50(1+2*0.0467) = 54.67 Hz

In the graph of the **current** (represented in the next image with marker labels for clarity), the sideband peaks are now visible, conversely with the no-load case, because the value of the slip is bigger, produced by an increment of the load. The sidebands are visible with a close approximation in frequency.

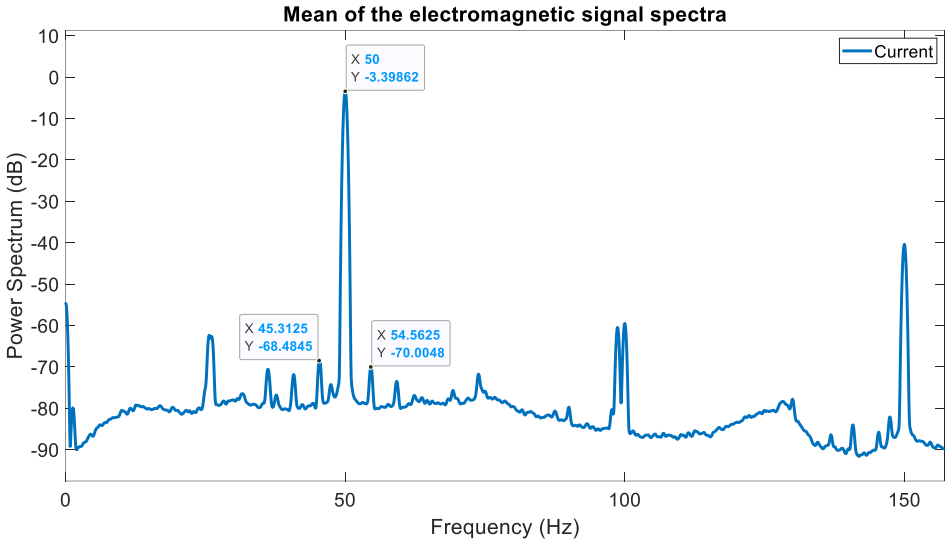

Figure 65: Frequency domain constant-load current

The values of the peaks under study for a broken bars analysis are reported in the next table.

	Frequency [Hz]	Magnitude [dB]	Magnitude difference between central peak and sidebands [dB]
Supply frequency	50	-3.39	
Left sideband	45.33	-68.48	65.1
Right sideband	54.67	-70.00	66.6

Table 15: Current constant-load values for Broken Rotor Bars

As can be seen in the table overhead, the magnitude differences, between the central peak and its sidebands, are very high in values (more than 60 dB) This, according to Thomson, is a symptom of a healthy motor, working under constant load conditions.

(Thomson & Gilmore, Motor current signature anaysis to detect faults in induction motor drives, 2003)

In the case of the **radial flux**, the frequency values of the broken bars–peaks, can be found at the same frequencies values calculated for the current signal. The next image represents the radial flux spectrum with the three peaks relative to the broken rotor bars analysis marked with labels.

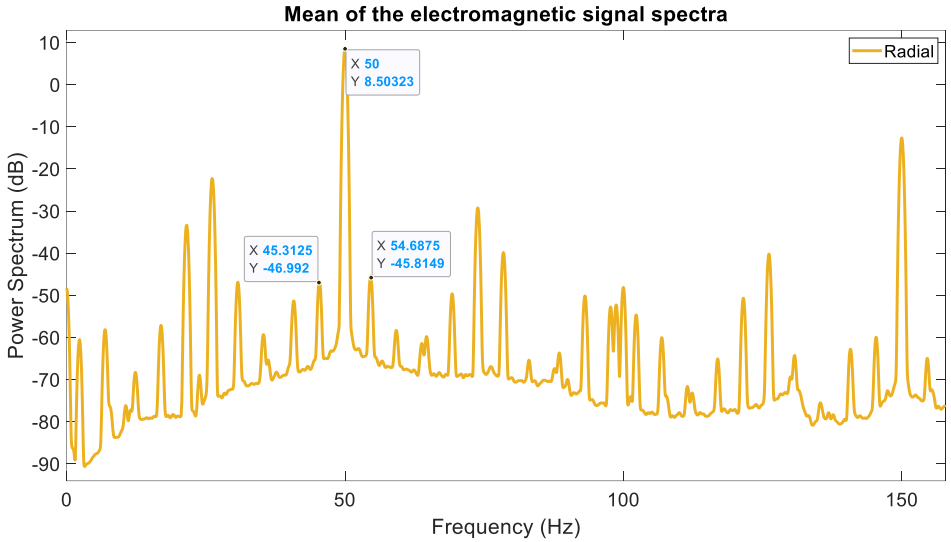

Figure 66: Frequency domain constant-load Radial flux

Though the paper (Thomson & Gilmore, Motor current signature anaysis to detect faults in induction motor drives, 2003),does not give any information on the magnitude difference between central and lateral peaks in stray flux signals (the work studies only the current signal), in this work a comparison of these magnitude differences will be carried out, to evaluate the efficacy of these kinds of signal for the broken rotor bar diagnostics.

It is assumed that the stray flux sensors are not displaced between one test and another.

The next table resumes the values of the peaks.

	Frequency [Hz]	Magnitude [dB]	Magnitude difference between central peak and sidebands [dB]
Supply frequency	50	8.50	

Left sideband	45.33	-46.99	55.49
Right sideband	54.67	-45.81	54.31

Table 16: Radial flux constant-load values for Broken Rotor Bars

The magnitude difference between the points indicated is also in this case more than the amplitude reference (for the current signal) of 26 dB. The differences are in this case slighthy less than in the current case (about 55 dB versus more than 60 dB in current signal). In any case, the magnitude difference between central and lateral peaks is still huge.

On the other hand, the values of the **axial flux** signal in frequency-domain are presented in the next picture, emphasizing the broken bars harmonics (marked with value labels).

The results obtained are close to that from the radial flux, though the sidebands are not symmetrical, with the right sideband lower in amplitude with respect to the left one. The values of the harmonics are reported in the next table.

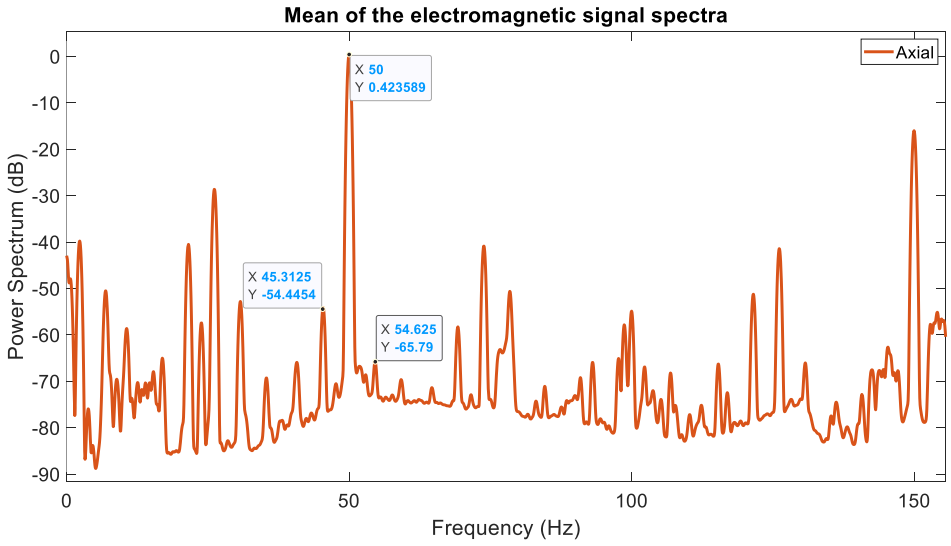

Figure 67: Frequency domain constant-load Axial flux

	Frequency [Hz]	Magnitude [dB]	Magnitude difference between central peak and sidebands [dB]
Supply frequency	50	0.42	
Left sideband	45.33	-54.44	54.86
Right sideband	54.67	-65.79	66.21

Table 17: Axial flux constant-load values for Broken Rotor Bars

As a partial conclusion, it can be said that, with a healthy machine, the difference between the magnitudes of the central and lateral peaks are very high (generally more than 50 dB) in both the current and flux signals.

In the next image the similarity between the two stray flux spectra is highlighted: As in the previous test, the values from the fluxes are very similar, and in general richer in harmonics than the current signal.

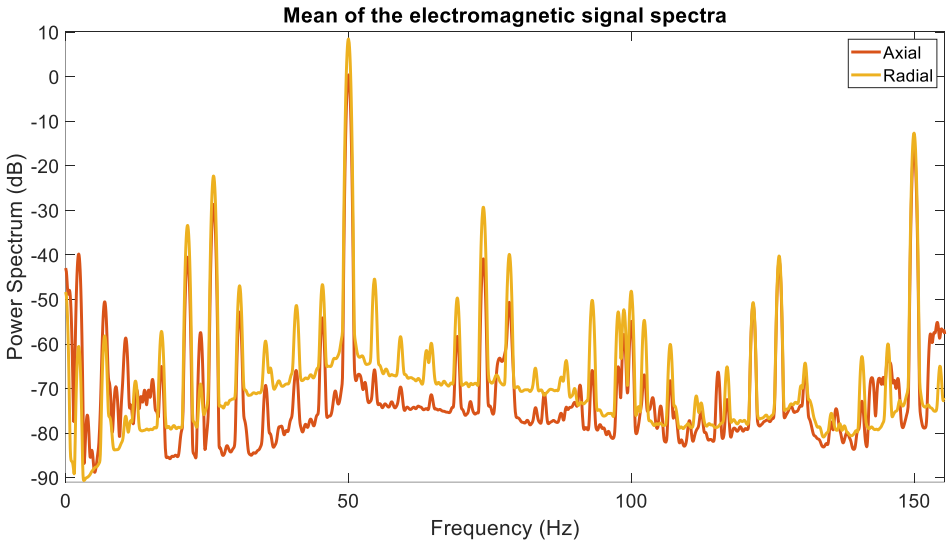

Figure 68: Frequency domain constant-load flux

5.3.3. Third Test: Variable Load, 5 Hertz

In the previous test, the excitation current to the brake and therefore the load to the motor were constant in time. Conversely in this test, the excitation current is going to be variable, giving the torque an oscillation in time. The frequency chosen for this test is 5 Hertz.

The voltage generated to control the current supplier of the brake, model BPM 103, is formed by two components: a mean voltage (constant component) of 2.5V, and an alternating component (sinusoidal) of 1V peak, with a frequency of 5Hz summed to the mean component.

The main condition extracted from the torque transducer software were:

- 1465 rpm (average mechanical speed of the rotor)
- 4.98 Nm (average braking torque)
- 520 W average braking power.

To control the BPM 103, a lower voltage has been selected than in the constant load condition, and in fact a lower excitation current is introduced into the brake, corresponding to a lower loading torque. With less torque, the result is an increment in the speed of the machine with respect to the previous case.

The values of the slip or those of the frequency are obtained with the same formulas presented in the previous test.

The obtained values are:

- f_1= Supply frequency, or frequency of the current stator winding: 50Hz
- f_2= Slip frequency, frequency of the current of the rotor: 1.17Hz
- f_m= Frequency of the movement of the rotor 24.41Hz
- s= Value of the slip 0.023

The results seen from the wattmeter are:

Motor's stator phase	Absorbed power	Absorbed current
Phase 1	277.76 W	2.78 A
Phase 2	318.52 W	2.92 A

Phase 3	314.97 W	2.73 A
Power Factor =0.437		

Table 18: Wattmeter variable-load (5 hertz)

As explained previously, applying less load to the machine induces the power factor and the active current to be lower in values, diminishing the electrical absorbed power of the machine.

5.3.3.1. Time Domain analysis

The following image shows the signals in time-domain.

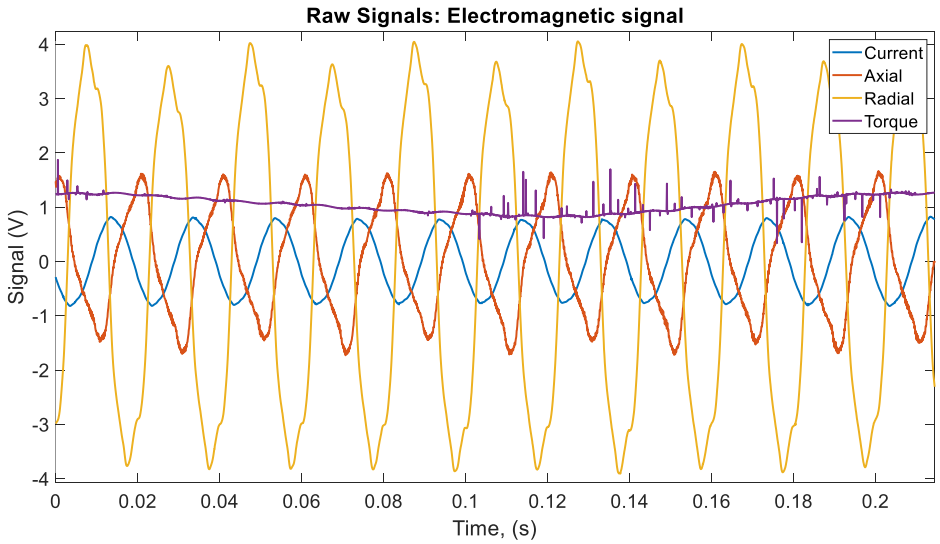

Figure 69: Time domain variable-load (5 hertz)

The graph shows how the **torque** experiments an oscillatory waveform because of the oscillating excitation current, impressed into the brake. Also, since the value of the control voltage is lower, the mean value of the torque signal has now decreased, having a value around 1.3 volts instead of the 2 volts of the previous experiment.

The period of the torque, according to the frequency selected, which can be seen in the Figure 69, is:

$$T = \frac{1}{f} = \frac{1}{5} = 0.2s \tag{43}$$

The **current** signal has a sinusoidal waveform taking values from -0.76 to 0.76 volts approximately.

In the figure below (Figure 70) the effect of the **current and the load torque** is highlighted, in a larger zoom. When the torque experiments an increase, the current from the grid does, and when the torque decreases, the current experiments a little decrease (this can be particularly observed looking at the shape of the envelope of the current signal). Resulting the current forming a shape of a wave, according to the frequency of the torque.

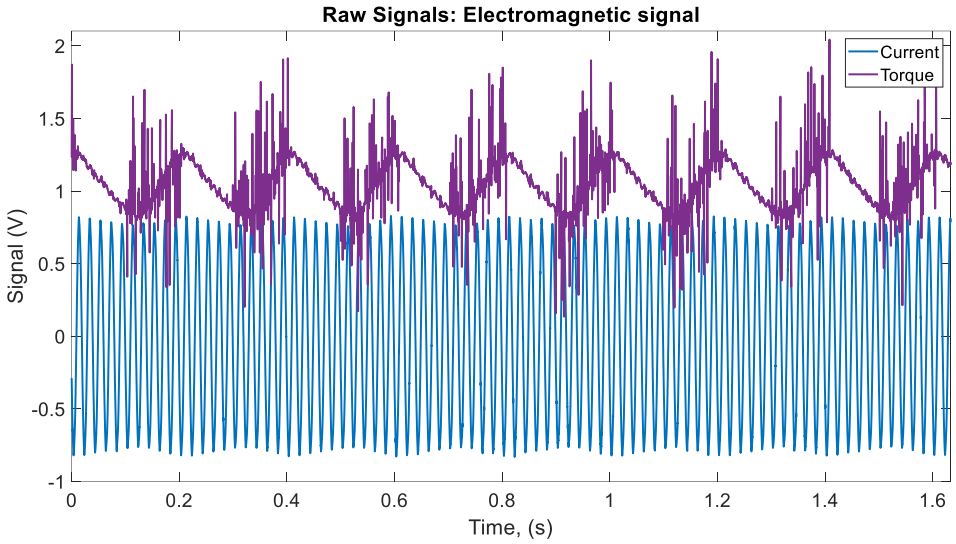

Figure 70: Time domain variable-load (5 hertz) current torque

Another thing that can be noted in the figure is that the torque signal does not have an alternating component perfectly sinusoidal, though the control signal does. This is probably due to the non-linear and multivariable torque-excitation current function of the magnetic hysteresis brake. Spikes in the torque signal can also be noted, that can be present probably due to measurements noise.

5.3.3.2. Frequency Domain analysis

Applying the Fourier transformation, the graph in the frequency domain for all the considered signals is:

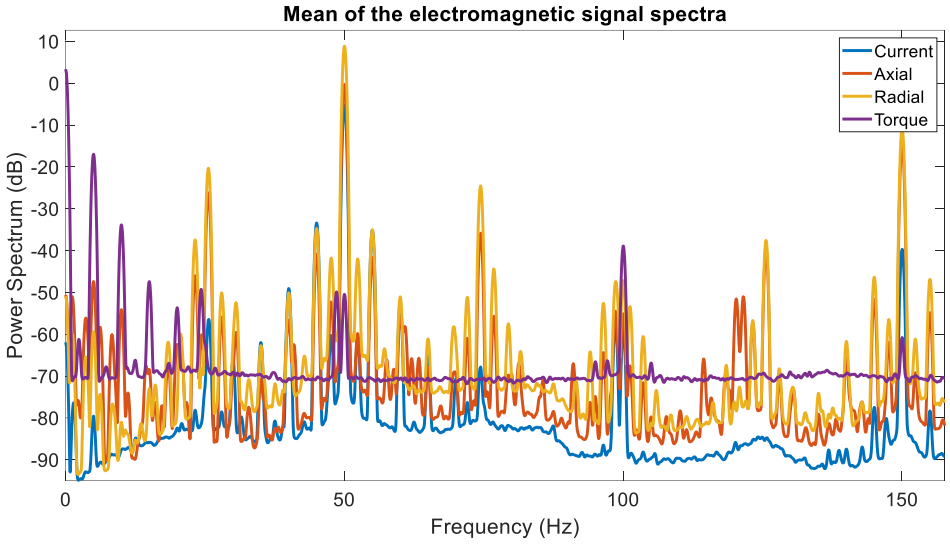

Figure 71: Frequency domain variable-load (5 hertz)

In this test, focalizing on the **torque** signal only, represented in the next figure, it can be seen that the torque-experiments a high value under the selected frequency, i.e. at 5Hz.

Also, can be seen in the graph, very prominent harmonics of the fundamental frequency at 10, 15 and 20 Hz. These harmonics are probably present due to the torque waveform non-perfectly sinusoidal, due to the non-linear characteristic of the hysteresis brake.

It is important to notice that the peak at 0 Hz is present, and reaches a magnitude above zero decibels, because of the mean value of the torque impressed.

As stated in the previous cases, probably due to some intrinsic degree of asymmetry in the motor, torque harmonics are again visible at the supply fundamental (50 Hz) and the 100Hz frequency.

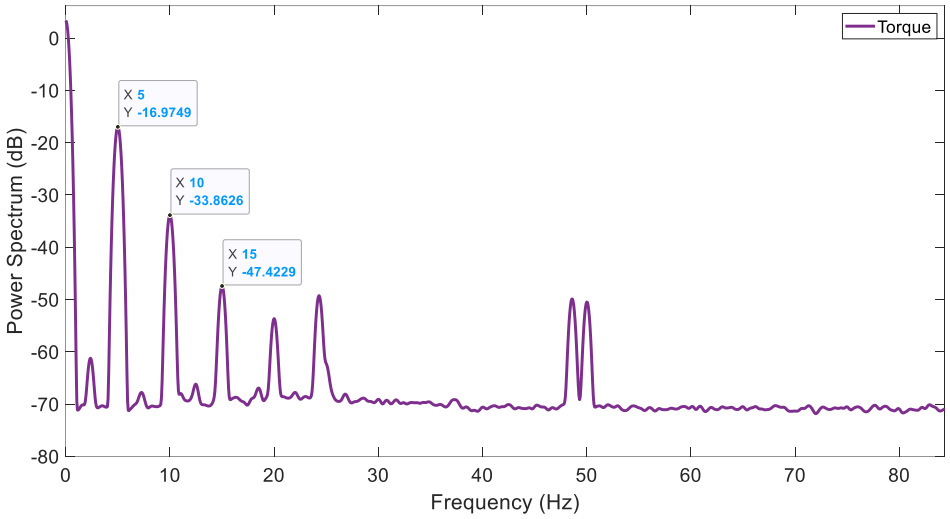

Figure 72: Frequency domain variable-load (5 hertz) Torque

Broken Rotor Bars analysis

To start studying the broken rotor bars, first is needed the value of the slip previously calculated, 0.023

Taking a look to the broken rotor bars phenomenon through the **current** (visible in the next figure), around the supply frequency (50Hz), there are more than a pair of sideband peaks. The closest ones are effect of the value of the slip (that is big enough to show the peaks), because a load is applied to the motor; and the other lateral peaks are effect of the selected oscillation frequency of 5 Hertz. Taking a look to these peaks, they are allocated exactly at 5Hertz on the sides of the supply frequency.

The first sideband peaks, due to the effect of the slip, i.e. due to the mean value of the torque, are located at:

- f_1= 50Hz
- left frequency= 50(1-2*0.023) = 47.7 Hz
- right frequency= 50(1+2*0.023) = 52.3 Hz

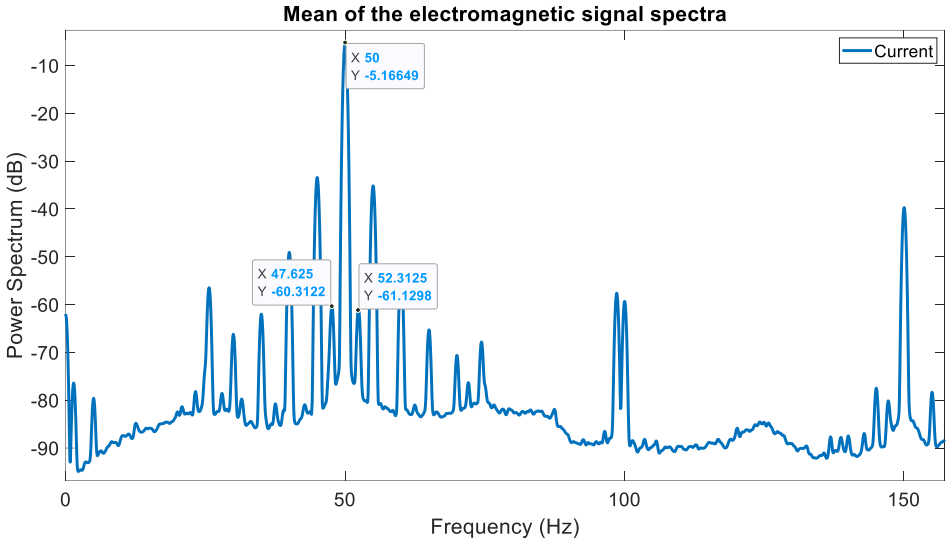

Figure 73: Frequency domain variable-load (5 hertz)-load current (I)

	Frequency [Hz]	Magnitude [dB]	Magnitude difference between central peak and sidebands [dB]
Supply frequency	50	-5.16	
Left sideband	47.7	-60.31	55.15
Right sideband	52.3	-61.12	55.96

Table 19: Current variable-load (5 hertz) values for Broken Rotor Bars (I)

Then, according to the theory previously explained, the amplitude experimented between these peaks is higher than 26 dB, which indicates a healthy motor.

On the other hand, the harmonics due to the torque oscillation are at the following frequencies (and highlighted with labels in the next figure):

- left frequency= 45 Hz

- right frequency= 55Hz

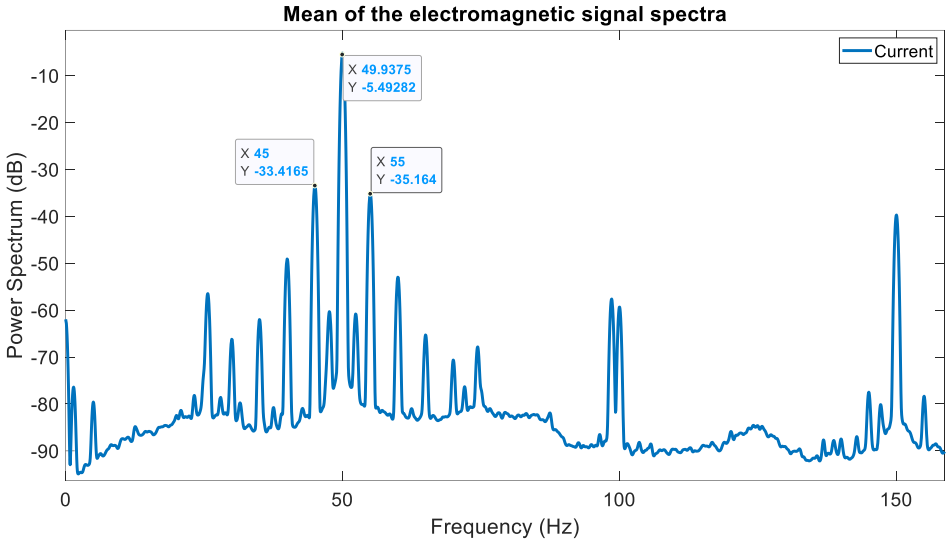

Figure 74: Frequency domain variable-load (5 hertz)-load current (II)

The harmonics assume the values reported in the table.

	Frequency [Hz]	Magnitude [dB]	Magnitude difference between central peak and sidebands [dB]
Supply frequency	50	-5.16	
Left sideband	45	-33.41	28.77
Right sideband	55	-35.16	30

Table 20: Current variable-load (5 hertz) values for Broken Rotor Bars (II)

As can be seen in the table above the peaks caused by the 5 hertz oscillation, give rise to a magnitude difference between central and sidebands slightly higher than 26 dB, specifically the difference is 30 dB, and 28.77 dB. This means, according to the document (Thomson & Gilmore, Motor current signature anaysis to detect faults in

induction motor drives, 2003), that there are no broken rotor bars, but the machine condition can be considered critical.

It is to be noted that, in actual facts it is known that the torque oscillations are in this case generated by the mechanical load (the brake) and not by the broken bars in the rotor. This in fact can be considered a false positive in the detection of broken bar. However, in any case, very high sidebands indicate that there is a high oscillating torque that can be due to a rotor bars fault, or a mechanical load with oscillating torque, e.g. reciprocating compressors.

Taking a look to the **radial flux** values, in the values shown in the table, the differences between the amplitudes of the peaks at the selected frequencies (due to the mean value of the slip), are not close to the 26dB threshold (they are around 50 dB). So, in this case, it can be said that the magnitude differences between central peak and sidebands, assumed by the current and radial stray flux signals are similar (the current sideband magnitude differences are around 54 dB).

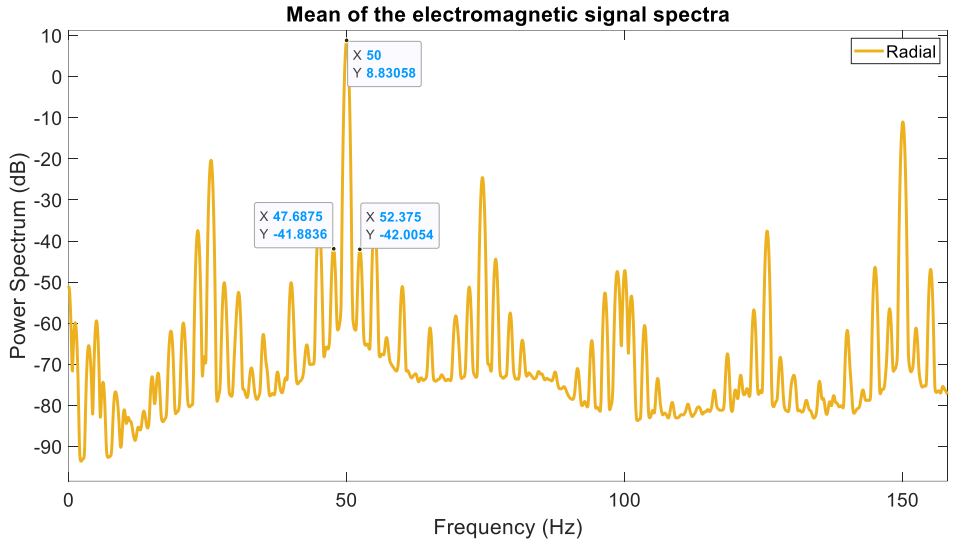

Figure 75: Frequency domain variable-load (5 hertz)-load Radial flux (I)

	Frequency [Hz]	Magnitude [dB]	Magnitude difference between central peak and sidebands [dB]
Supply frequency	50	8.83	

Left sideband	47.7	-41.88	50.71
Right sideband	52.3	-42.00	50.83

Table 21: Radial flux variable-load (5 hertz) values for Broken Rotor Bars (I)

There are also the lateral bands caused by the frequency of 5 Hertz. The harmonics are visible in the next figure with their values that are resumed in the following table.

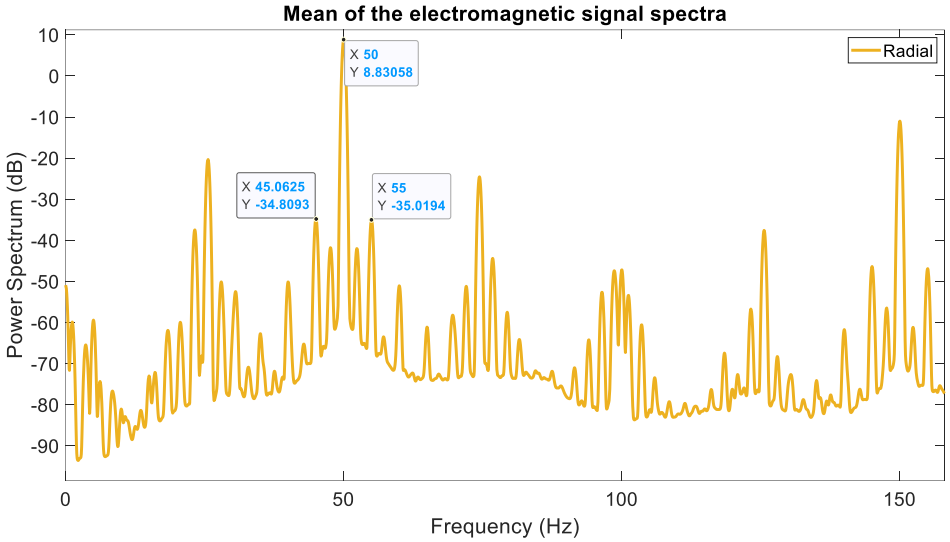

Figure 76: Frequency domain variable-load (5 hertz)-load Radial flux (II)

	Frequency [Hz]	Magnitude [dB]	Magnitude difference between central peak and sidebands [dB]
Supply frequency	50	8.83	
Left sideband	45	-34.80	43.63
Right sideband	55	-35.02	43.85

Table 22: Radial flux variable-load (5 hertz) values for Broken Rotor Bars (II)

The difference between these peaks is more critical than that of the peaks due to the mean value of the slip measured above (around 43 dB versus 50 dB of the peaks due to the mean value of the slip). Moreover, confronting these values with that of the constant load case (5.3.2), it can be noted that the peaks are more severe in this case, since the magnitude difference of the constant load case was about 54-55dBs.

Though there is not exactly a value, for the flux signal, of the threshold of the magnitudes of the sidebands for diagnosing the broken rotor bars, with an oscillation torque, the sidebands magnitude increases, with respect to the central peak, as studied in the tables above.

Considering the values of the **axial flux**, the results obtained are a little different from that of the radial flux. In fact, it can be noted that the sidebands are not symmetrical in this case, especially for the sidebands due to mean value of the load. The peaks are visible in the next figure.

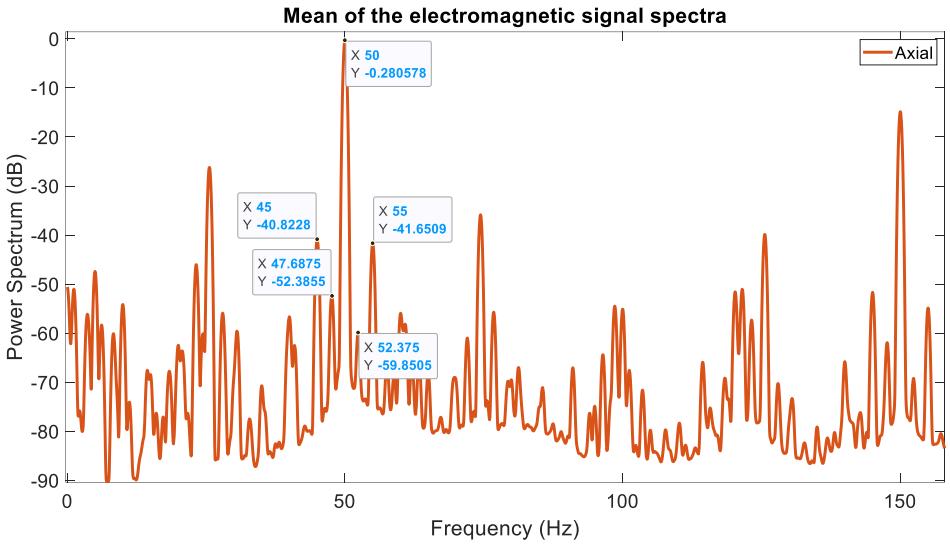

Figure 77: Frequency domain variable-load (5 hertz)-load Axial flux (I)

The table with the values of the lateral peaks, due to the mean load, is in the following:

	Frequency [Hz]	Magnitude [dB]	Magnitude difference between central peak and sidebands [dB]
Supply frequency	50	-0.208	

Left sideband	47.7	-52.29	52.08
Right sideband	52.3	-59.93	59.72

Table 23: Axial flux variable-load (5 hertz) values for Broken Rotor Bars (I)

Though there is no specific threshold for the flux signal, the amplitude differences can be considered big enough to consider the motor without any problems. The values moreover are similar to that of the constant load condition.

The table with the values of the peaks due to the frequency oscillation is the following:

	Frequency [Hz]	**Magnitude [dB]**	**Magnitude difference between central peak and sidebands [dB]**
Supply frequency	50	-0.28	
Left sideband	45	-40.91	40.63
Right sideband	55	-41.65	41.37

Table 24: Axial flux variable-load (5 hertz) values for Broken Rotor Bars (II)

In this case, the magnitude difference is smaller (from a difference around 55 dB to 40 dB one), indicating that, also in radial flux, the amplitudes of the sidebands increase when a torque oscillation occurs.

5.3.4. Fourth test: Variable Load, 2 Hertz

This last test is going to be realized with similar conditions as the previous one, where the excitation current is variable in time, giving the torque an oscillation in this case of 2 hertz.

The other conditions applied to this test are the mean voltage of 2.5V to the BPM 103, with an oscillating component with amplitude peak of 1V.

The value extracted from the LabVIEW torque transducer program was the mechanical speed of the rotor, with a mean value of 1470 rpm.

The values of the wattmeter are:

Motor's stator phase	Absorbed power	Absorbed current
Phase 1	247.04 W	2.898 A
Phase 2	290.21 W	2.931 A
Phase 3	314.48 W	2.661 A
Power Factor =0.497		

Table 25: Wattmeter variable-load (2 hertz)-

The values of the slip or those of the frequency are obtained with the same formulas that are presented in the previous test.

The obtained values are:

- f_1= Supply frequency, or frequency of the current stator windings: 50Hz
- f_2= Slip frequency, frequency of the current of the rotor: 1Hz
- f_m= Frequency of the movement of the rotor 24.5Hz
- s= Value of the slip 0.02

5.3.4.1. Time Domain analysis

The time domain graph shown results similar to that of 5Hz, with the difference of the frequency of the torque, making longer the value of the period.

$$T = \frac{1}{f} = \frac{1}{2} = 0.5s \tag{44}$$

Also, as in the last case examined, the torque experiments more noise (spikes) in the increasing part of the waveform, rather than the decreasing one (as visible in Figure 78).

The values of the **current** are modified according to the demanded torque, resulting an oscillating shape for the current. As in the case of the 5 Hz oscillation the amplitude values of the current increase a little during the increasing fronts of the waveform of the torque and decrease during the decreasing fronts. This fact slightly modifies the envelope of the current signal as in the previous case of the 5 Hz oscillation.

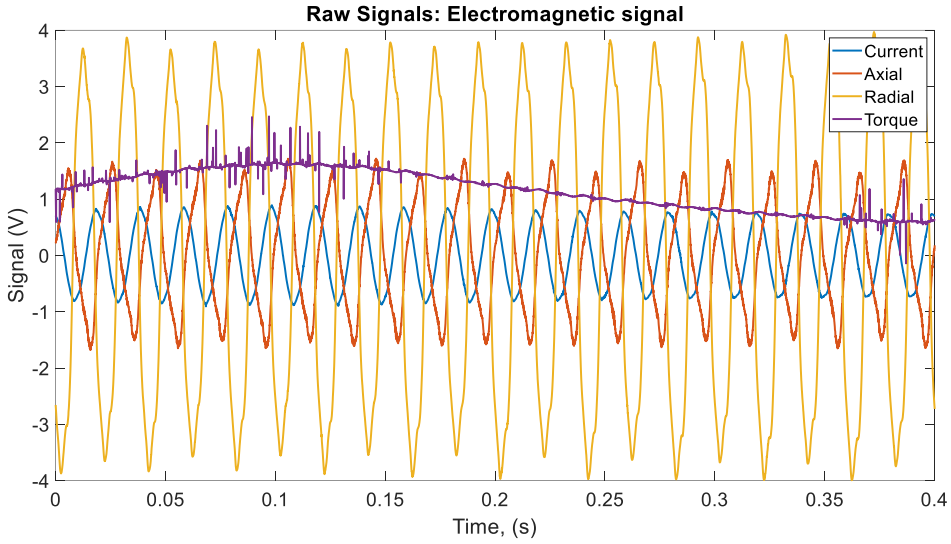

Figure 78: Time domain variable-load (2 hertz)

5.3.4.2. Frequency Domain analysis

The next image represents an overview of all the considered signals in frequency domain. As usual, the highest peaks for the electromagnetic signals are at the supply frequency and its odd multiples, though many sidebands have quite high values.

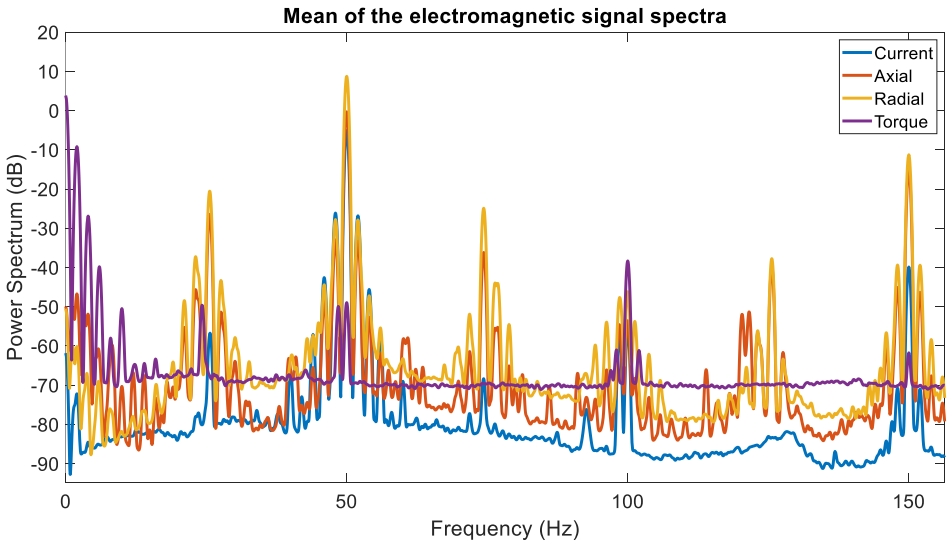

Figure 79: Frequency domain variable-load (2 hertz)

In, the analysis of the **torque** signal in the frequency domain (reported in the next figure), the peak at 2 Hz can be easily seen, that is the selected working frequency; also, as in the previous case of the 5 Hz oscillation, the harmonics of the fundamental at 2 Hz (both odd and even) are quite prominent, denoting the torque is not perfectly sinusoidal.

From the graph it is also possible to see high value around the 0 Hz (with a peak of about 3 dB magnitude), which represents the mean value of the torque load signal.

Thus, it confirms that the torque peaks at 0 Hz gets higher values when a load is applied.

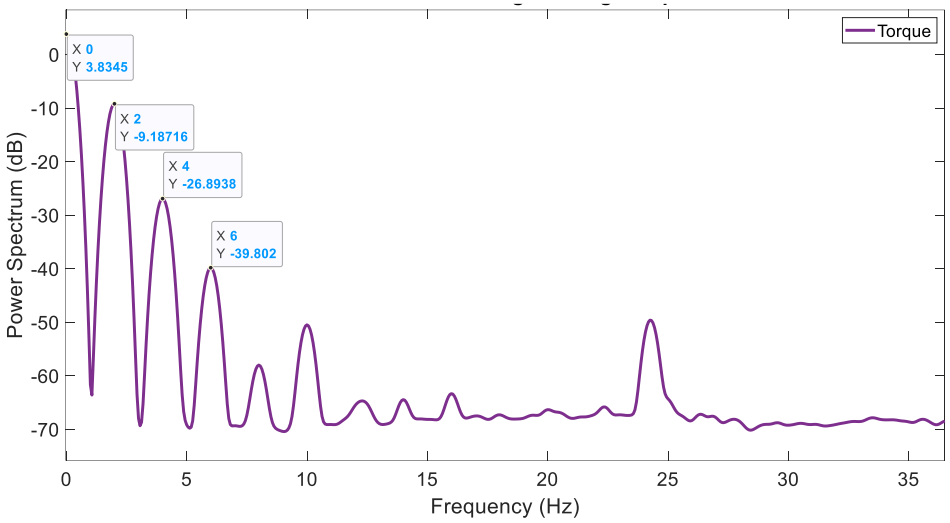

Figure 80: Frequency domain variable-load (2 hertz) Torque

Broken Rotor Bars analysis

To determine the broken bars phenomenon, in the analysis of 2 Hertz condition, the value of the slip is needed, previously calculated, 0.02.

In this case of the frequency domain, against the previous one, the peaks that would appear as a cause of the frequency selected are the same obtained as those that occur of the effect of the load, thanks to the value of the slip.

This means, that the important peaks that are going to be studied for this phenomenon are summed between them, and are the closest ones to the supply frequency.

The calculated frequencies are the following:

- f_1= 50Hz
- left frequency= 50(1-2*0.02) = 48 Hz
- right frequency= 50(1+2*0.02) = 52 Hz

The analysis in the **current** spectra (shown in the next figure), at the calculated frequencies, clearly shows a fault in the broken rotor bars phenomenon or load oscillation anomaly; this because the amplitude difference between the studied peaks

is critical, being a difference between them less than 26dB (it is about 21-22 dB, as resumed in the following table).

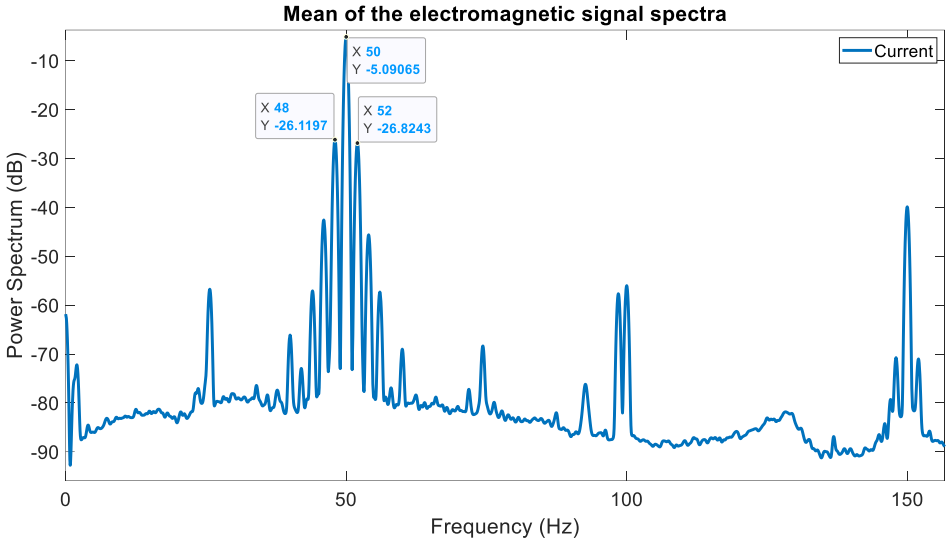

Figure 81: Frequency domain variable-load (2 hertz)-load current

	Frequency [Hz]	Magnitude [dB]	Magnitude difference between central peak and sidebands [dB]
Supply frequency	50	-5.09	
Left sideband	48	-26.11	21.02
Right sideband	52	-26.82	21.73

Table 26: Current variable-load (2 hertz) values for Broken Rotor Bars

In the graph of the **radial flux** (represented in the next figure), the difference between the indicated points is around 36 dB in the amplitude, as reported in the next table. The values of the sidebands relative to central peak have increased with respect to all previous cases, showing that also in the radial stray flux signal, in a more severe condition the trend of this feature increases.

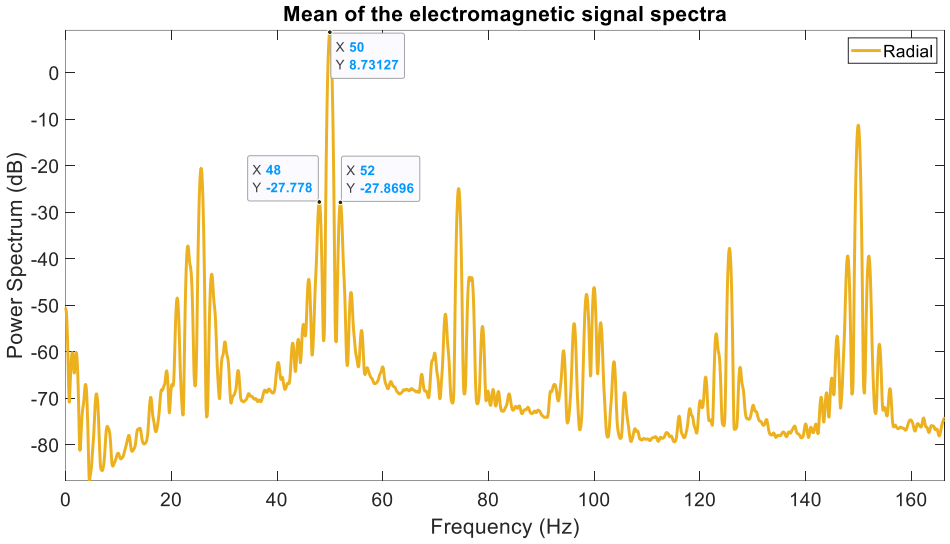

Figure 82: Frequency domain variable-load (2 hertz)-load Radial flux

	Frequency [Hz]	Magnitude [dB]	Magnitude difference between central peak and sidebands [dB]
Supply frequency	50	8.73	
Left sideband	48	-27.77	36.5
Right sideband	52	-27.86	36.6

Table 27: Radial flux variable-load (2 hertz) values for Broken Rotor Bars

In this case, **the axial flux** experiments a little magnitude difference between the peaks selected. The spectrum and the values of the peaks are visible in the next figure and table. Again, as in the case of the radial flux, with this signal, though it is not possible to stabilize an effective threshold, it can be noted that, in this case in which the current signal gives the worst results, the sidebands are increased in magnitudes (relatively to the central peak) more than that of all previous cases.

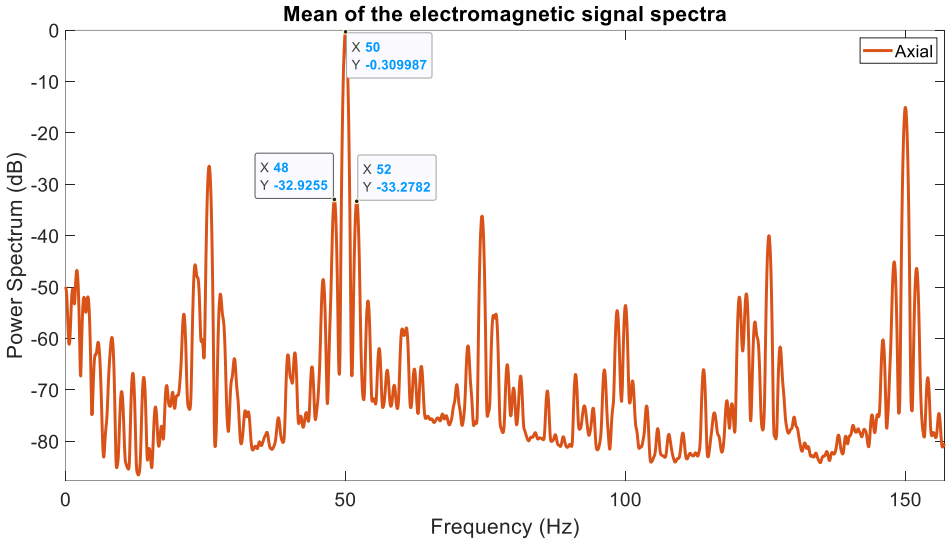

Figure 83: Frequency domain variable-load (2 hertz)-load Axial flux

	Frequency [Hz]	Magnitude [dB]	Magnitude difference between central peak and sidebands [dB]
Supply frequency	50	-0.30	
Left sideband	48	--32.92	32.62
Right sideband	52	-33.27	32.97

Table 28: Axial flux variable-load (2 hertz) values for Broken Rotor Bars

As explained previously, in the 5Hz case, the torque oscillations (signal of a faulty motor), can be caused by the broken rotor bars, or by an oscillation in the mechanical load. In these two last experiments, the torque oscillations are coming from an oscillating load; in actual situations this torque oscillation can be interpreted as broken rotor bars, though they are not, so constituting a false positive in the diagnosis of broken bars.

6. CONCLUSIONS AND RESULTS

This chapter presents the conclusions drawn from the results shown in the previous chapters.

In order to be able to analyze the spectral representations of the different signals, a preliminary study was carried out, to acquire the basic knowledge of the Fourier Transform and its different variants. Also, the implementation of this algorithm into a MATLAB software, through the *pspectrum* function, is reported.

The reason why the **values into the frequency domain** are close to -90dB becomes from the conversion into decibels. The values that are close to zero, are equivalent to -90dB (logarithm function). Taking a close look to the torque, for example, the values in the time domain were approximately zero; and in the harmonic signal the values are close to -90dB.

The **value of the torque** in decibels, as seen in the frequency domain, gets higher values, when a load is applied. The difference is huge, because the value without load was around -40 decibels; but the value with any load condition was always close to zero decibels (into the frequency domain). This difference can also be seen in the time domain, where the value of no-load condition was zero volts, and in other cases the value of the torque takes higher values than zero.

It can be noted, moreover, that the **axial flux**, **compared to the radial one**, is richer in harmonics; this can be attributed to the fact that the axial flux probe probably collects more magnetic field from the end windings of the machine; conversely, the radial flux should be more similar to the airgap flux, since the end-winding field should not influence it too much due to the distance between it and the probe. In other words, the radial signal should be less rich in harmonics or more sinusoidal.

The **values of the wattmeter**, where each of the three channels of the three-phase motor are presented, represent the absorbed power and current from the grid, according to the necessities of the motor. Taking a look to the values of the absorbed current, they increment with the value of the braking torque. As more load is selected, the current needed by the motor is bigger. Also, where there is an oscillation of the mechanical load, the values of the current are lower, because the mean torque applied by the brake is minor.

6.1. Broken rotor bars phenomenon.

The following table shows the results obtained from the different tests, to examine the Broken Rotor Bars phenomenon, carried out on the studied motor. The results obtained, studying the current and the flux, are reported in this table:

	No load	Constant load	5Hz load		2Hz load
			load	5hz	
Current	x	Healthy	Healthy	Healthy	False positive
Radial Flux	x	Healthy	Healthy	x	x
Axial Flux	x	Healthy	Healthy	x	x

Table 29: results from broken rotor bars

In Table 29, there are results denoted with an (x) element, denoting there is no certain outcome.

1) The first conclusion obtained concerns the slip, in this analysis the peaks are more visible as the load increases. This is result of the slip.

   The slip increases as the load does, because when a load is applied, the mechanical frequency of the rotor decreases, and the frequency of the current of the rotor increases. According to the formula that links both frequencies of the currents, and knowing that the one from the stator is constant (f_1= 50 Hz):

$$f_2 = sf_1 \tag{45}$$

   This slip marks higher values (with load), making greater difference between the 50 Hz frequency and the peaks that can appear next to it.

   As shown in the text, at no load, the peaks to study this phenomenon due to the low value of the slip cannot be seen, as the ones when the slip took higher values.

2) As a second conclusion, it can be said that the trend of these sidebands, for both stray fluxes, can be studied for diagnosing broken rotor bars or oscillation torque effects of the mechanical load. However, it has to be remembered that the position of the sensor should not change between the various measurements since the spectra signatures can change a lot with different positions of the sensors.

3) A third conclusion is about the graphs with a frequency applied to the load condition; what can be seen, in the test realized with oscillating torque frequency,

is that the sideband peaks, due to the frequency selected, are more pronounced rather than those caused by the load.

4) In the table related to the case at 2Hz, some results are false-positive. This is caused by the mechanical load (the brake), creating an oscillating torque, and inducing into a faulty motor, when in reality the motor is completely healthy.

7. ANEX

7.1. Data Table

The following statement is to illustrate the table used to carry out some of the values to examine different characteristics and parameters of the motor, and also, to reflect some of the results applied to the theory.

The values of this table have been taken in the test bench, with a motor RAEL RL 90L 4, in the laboratory of the University of Pavia, in Italy.

Since the values are taken by hand from the results given from the different programs such as MATLAB or LABVIEW, these parameters always have an uncertainty.

Aside, one of the values taken by hand from the power factor in the wattmeter, did not correspond with the other ones, making a big difference between its previous and its following values. Because of this, to regulate the value a linear interpolation has been done.

To realize this linear approximation, the formula is:

$$y = y_1 + \frac{(y_2 - y_1)}{(x_2 - x_1)}(x - x_1) \tag{46}$$

The table of values used to get the value is:

Rotor speed (rpm)	PF
1467.8	0.379
1461.9	y
1459.1	0.49

Table 30: Interpolation table

$$y = 0.379 + \frac{(0.49 - 0.379)}{(1459.1 - 1467.8)}(1461.9 - 1467.8) = 0.4554 \quad (47)$$

The result, given by the formula (*47*), is the value taken for the power factor to analyze the test done.

Voltage [V]	rotor speed [rpm]	Torque [Nm]	Power [W]	P1 [W]	P2 [W]	P3 [W]	PF	Pin [W]	Efficiency	slip	rotor speed (rad/s)
0	1497,6	0,029	10	65,54	101,75	95,7	0,107	262,99	3,80%	0,16%	156,8283053
0,5	1493,8	0,13	25,1	71,39	105,15	100,75	0,116	277,29	9,05%	0,41%	156,4303702
1	1492,1	0,439	71,4	85,27	121,79	114,52	0,14	321,58	22,20%	0,53%	156,2523466
1,5	1488,4	0,95	154	117,24	152,31	142,82	0,191	412,37	37,35%	0,77%	155,8648835
1,8	1484,6	1,55	242	143,83	179,4	171,12	0,233	494,35	48,95%	1,03%	155,4669485
2	1480,5	1,98	313	166,5	203,49	194,43	0,271	564,42	55,46%	1,30%	155,0375975
2,2	1477,5	2,51	380	193,33	231,77	222,07	0,312	647,17	58,72%	1,50%	154,7234382
2,4	1472,3	3,10	474	223,45	264,07	253,09	0,359	740,61	64,00%	1,85%	154,1788955
2,6	1467,8	3,78	580	260,09	301,09	289,61	0,379	850,79	68,17%	2,15%	153,7076566
2,8	1461,9	4,55	704	300,65	342,53	329,76	0,4554	972,94	72,36%	2,54%	153,08981
2,9	1459,1	4,9	750	320,9	361,5	350,7	0,49	1033,1	72,60%	2,73%	152,7965947

3	1455,5	5,3	806	343	387,9	375,6	0,519	1106,5	72,84%	2,97%	152,4196036
3,1	1451,2	5,8	875	370,6	413,2	403,5	0,55	1187,3	73,70%	3,25%	151,9693086
3,2	1446,5	6,249	959	397,36	444,1	433,11	0,58	1274,57	75,24%	3,57%	151,4771258
3,3	1442,6	6,9	1040	429,61	473,45	490	0,6	1393,06	74,66%	3,83%	151,0687187
3,4	1436,8	7,39	1109	460,79	504,75	495,19	0,639	1460,73	75,92%	4,21%	150,4613442
3,5	1431,83	8,026	1186	493,11	541,33	528,15	0,66	1562,59	75,90%	4,54%	149,940887
3,6	1425	8,56	1289	530,77	575,7	562,66	0,692	1669,13	77,23%	5,00%	149,225651
3,7	1420	9,27	1356	566,92	614,16	599,88	0,717	1780,96	76,14%	5,33%	148,7020523
3,8	1412	9,8	1460	605,71	654,06	640,05	0,74	1899,82	76,85%	5,87%	147,8642942
3,9	1405,5	10,46	1545	646,4	695,37	680,12	0,764	2021,89	76,41%	6,30%	147,1836158
4	1398	11,2	1642	689,1	737,11	723,24	0,785	2149,45	76,39%	6,80%	146,3982177

7.2.Filter modifications

Since the signal obtained from the MEMS (to analyze the vibration) was not accurate, some changes from the filter has to be made to evaluate a better signal.

The component to work with is the EVAL-ADXL335Z, a device from the ANALOG DEVICES, with dimensions of (200mm* 20mm), described as a simple evaluation board, with four capacitors of 100nF.

The first capacitor C1 is a bypass to reduce supply noise. The capacitors like C2, C3, C4 are filter capacitors to set a bandwidth of 50 Hz. In the case that a bigger bandwidth is needed, these three last capacitors can be changed as appropriate.

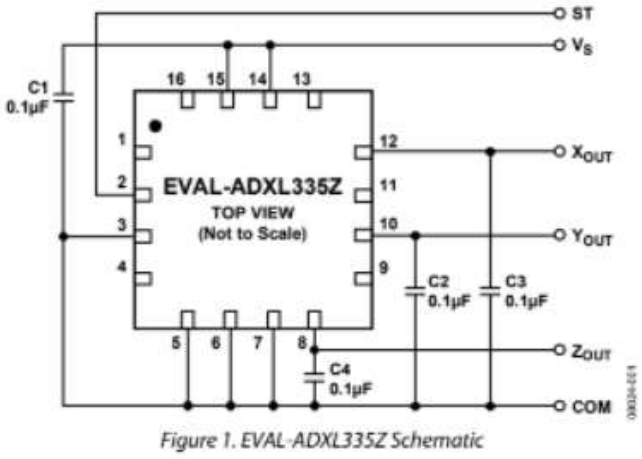

Figure 84: Schematic EVAL-ADXL335Z

Some of the results done with the bandwidth of 50Hz showed that the signal obtained was not enough, because the signals were truncated, and they did not represent any clear values. Because of that, the values of the capacitors were changed. According to the datasheet, the maximum value acceptable for a bandwidth in X or Y direction is 1600Hz, and 550 Hz in the Z direction.

Using the formula given in the datasheet to calculate the new capacities, we obtain:

$$F_{-3\,\mathrm{dB}} = 5\ \mu\mathrm{F}/C_{(X,Y,Z)} \tag{48}$$

- X, Y Axis (1500Hz), 3.3nF
- Z Axis (500Hz), 10nF

Normally, only the values used are those of the X and Y axis, that can tolerate higher values. (ANALOG DEVICES, 2009)

7.3.Hot Spots

The nucleus of the stator in the induction motors, is composed by metal sheets insulated between them, with the purpose to eddy parasite currents. When this insulation damages, it produces an interlaminar injury, which brings an increase in the circulation of the eddy currents, and an increase in the temperature of the core, forming hot spots. (de la Barrera, Solsona, García, Curti, & Bossio, 2007)

8. Bibliography

Aexander, C., & Sadiku, M. (s.f.). *Fundamentos de circuitos eléctricos.* Mc Graw Hill.

Alvizu, G. (junio de 2022). *Clasificacion de Motores Electricos segun NEMA.* Obtenido de https://studylib.net/doc/25539824/clasificacion-de-motores-electricos-segun-nema

ANALOG DEVICES. (2009). *Three-Axis Accelerometer Evaluation board.*

Asociation for advancing automation. (june de 2022). *The Hysteresis Loop & Testing Permanent Magnet Materials*. Obtenido de https://www.automate.org/blogs/the-hysteresis-loop-and-testing-permanent-magnet-materials

Causas, diagnósticos y medidas preventivas. (1994). En H. Enrique Peña, C. Hernando Ramirez, & E. Mahecha Ledezma, *Fallas en los Motores Eléctricos de Inducción.*

Compact Air. (n.d.). Oil free piston compresors.

DATADEC. (2022, April). *MANTENIMIENTO PREVENTIVO VS CORRECTIVO*. Retrieved from https://www.datadec.es/blog/mantenimiento-preventivo-vs-correctivo

de la Barrera, P., Solsona, J., García, G., Curti, M., & Bossio, G. (2007, March). *Un método para la generación de fallas en el hierro del estator de los motores de inducción.* Córdoba. Retrieved from https://www.researchgate.net/publication/229018568_Un_metodo_para_la_generacion_de_fallas_en_el_hierro_del_estator_de_los_motores_de_induccion

de la Torre, F. (s.f.). *Accionamientos Electromecánicos.*

Fernández Villafañez, J. I. (2018). *Diagnóstico de fallos en rodamientos de motores eléctricos mediate tecnicas lasso.* Valladolid.

Fraile Mora, J. (2003). *máquinas electéctricas.*

Frosini, L. (2022). *Il motore asincrono: principi di funzionamento.* Pavia.

García Santamaría, C. (2017). *Análisis espectral de señales para la detección de fallos de motores de inducción.*

González Sánchez, J. (2022). *Conceptos de control por computador.* Valladolid.

Gritli, Y. (2014). *Diagnosis and Fault Detection in Electrical Machines and Drives based on Advanced Signal Processing Techniques.*

IBERDROLA. (April de 2022). *Mantenimiento predictivo: la técnica basada en datos clave para anticipar errores*. Obtenido de https://www.iberdrola.com/innovacion/mantenimiento-predictivo

Lee, S. B. (2021). *Overview of Testing and Condition Monitoring of Induction and Synchronous Machines in an Industrial Environment.*

López Tello, J., & Bedoya Arango, J. (1997). *Fallas en el rotor del motor de inducción tipo jaula de ardilla.*

Magnaghi, M. (2015). *STRUMENTI DIAGNOSTICI PER L'INDIVIDUAZIONE DI GUASTI DI STATORE E DEI CUSCINETTI NEI MOTORI ASINCRONI.* Pavia.

MAGTROL. (s.f.). brakes & clutches.

MAGTROL. (s.f.). TS SERIES. *IN-LINE TORQUE SENSORS*.

Malcovati, P. (s.f.). *Misure Elettriche.*

Martín-Riva, P. M.-O. (2014). *CONCEPCIÓN DE UN MOTOR ASÍNCRONO DE JAULA DE ARDILLA.*

Moríñigo Sotelo, D., Pons Llinares, J., & Fernandez Cavero, V. (2021, august). *Spectral analysis of stationery and transient signals for monitoring of electrical machines*. Retrieved from https://uvadoc.uva.es/handle/10324/52314

MRO Machinery and equipment . (2022, May). *Maintenance, Reliability and Operations*. Retrieved from https://www.mromagazine.com/features/troubleshooting-rolling-element-bearings/

RAEL. (s.f.). RAEL MOTORI ELETTRICI.

Research Gate. (May de 2022). Obtenido de https://www.researchgate.net/figure/A-typical-roller-bearing-showing-different-component-part-1_fig1_337933015

RKB. (2010). *THE MOST COMMON CAUSES OF BEARING FAILURE AND THE IMPORTANCE OF .* Retrieved from https://pdf.directindustry.com/pdf/rkb-europe/most-common-causes-bearing-failure-importance-bearing-lubrication/27918-138476.html

Rodíguez Pozueta, M. (2018). *Máquinas Eléctricas 2.*

SCHULICH SCHOOL OF ENGINEERING. (2022, june). *Electric machines*. Retrieved from STANDARDS AND LEGISLATION: https://people.ucalgary.ca/~aknigh/electrical_machines/induction/i_standard.html

Tecnológico de Monterrey. (n.d.). *Energía eléctrica: Introducción y conceptos básicos.*

The engineer toolbox. (2022, Junio). *NEMA A, B, C and D Electrical Motor Design*. Retrieved from https://www.engineeringtoolbox.com/nema-a-b-c-d-design-d_650.html

Thomson, W., & Culbert, I. (s.f.). *Current Signature Analysis for Condition Monitoring of Cage Induction Motors: Industrial Application and Case Histories.*

Thomson, W., & Gilmore, R. (2003). *Motor current signature anaysis to detect faults in induction motor drives.* Scotland.

WIKIBOOKS. (2022, June). *Magnetic hysteresis*. Retrieved from https://it.wikibooks.org/wiki/File:Magnetic_hysteresis.png

Wikipedia. (2022, May). *Corona discharge*.

WIKIPEDIA. (2022, March). *Fourier transform*. Retrieved from https://en.wikipedia.org/wiki/Fourier_transform

WIKIPEDIA. (2022, Mrch). *Magnetic flux*. Retrieved from https://en.wikipedia.org/wiki/Magnetic_flux